NUCLEAR CALCIUM DYNAMICS IN HIPPOCAMPAL NEURONS

by

Aram Abbasian

Submitted in partial fulfilment of the requirements
for the degree of Master of Science

at

Dalhousie University
Halifax, Nova Scotia
July 2016

TABLE OF CONTENTS

LIST OF FIGURES

ABSTRACT

Increasing evidence points to neuronal nuclear calcium signalling as a conduit between electrical activity and transcription-dependent changes, and it is possible that different mechanisms of nuclear calcium influx trigger distinct genomic responses. Therefore, detailed analysis of these mechanisms is a critical step in understanding nuclear calcium function. We imaged spontaneous cytosolic and nuclear calcium transients and found that nuclear transients decay more slowly, facilitating calcium build-up in the nucleus more readily during rapid trains of transients. To determine whether nuclear transients were dependent on perinuclear calcium release, we inactivated sarco/endoplasmic reticulum calcium ATPase (SERCA) pumps, ryanodine receptors (RyRs) and IP_3 receptors (IP_3Rs), and found that these manipulations did not have an effect, indicating that nuclear elevations were driven primarily by diffusion of cytosolic calcium through nuclear pores. Finally, by blocking IP_3R activation, we demonstrated that RyRs can propagate calcium waves to the nucleus independent of IP_3Rs.

LIST OF ABBREVIATIONS AND SYMBOLS USED

AChR	Acetylcholine receptor
AMPAR	α-amino-3-hydroxy-5-methyl-4-isoxazolepropionic acid receptor
CaM	Calmodulin
CaMK	Ca^{2+}/calmodulin-dependent protein kinase
CICR	Calcium-induced calcium release
EPSP	Excitatory postsynaptic potential
ER	Endoplasmic reticulum
GABA	γ-Aminobutyric
GECI	Genetically-encoded calcium indicator
GluR	Glutamate receptor
HFS	High frequency stimulation
IP_3	Inositol 1,4,5-trisphosphate
IP_3R	Inositol triphosphate receptor
LTP	Long-term potentiation
MAM	Mitochondria-associated membrane
MCU	Mitochondrial calcium uniporter
NCX	Sodium-calcium exchanger
NE	Nuclear envelope
NMDAR	*N*-methyl-D-aspartate receptor
NPC	Nuclear pore complex
PKA	Protein kinase A
RyR	Ryanodine Receptor

SERCA	Sarco/endoplasmic reticulum calcium ATPase
θ	Theta
τ	Tau
TBS	θ-burst stimulation
VGCC	Voltage-gated calcium channel
XeC	Xestospongin C

ACKNOWLEDGEMENTS

I am forever indebted to my supervisor, Dr. Alan Fine, not just for the experience he has allowed me to take away from this past year spent completing this thesis, but for everything he has given me during my time as a student in his lab over the last three and a half years. Having started out in the lab as an undergraduate student simply looking to see research up close, I am now leaving with a new passion and professional objective towards which to strive - the rarity of such transformative experiences is not lost on me. Dr. Fine's wisdom and guidance have been fundamental to my growth since I first started, and his endless support, be it in lab-related matters or otherwise, and caring personality are part of what made the process a joy. The impact this experience has had on me is permanent, as is my gratitude towards him.

To Dr. Baldridge, Dr. Croll, Dr. Barnes, and Dr. Quinn, I express my most sincere gratitude not just for their professional contribution as committee members, but also for acts of patience and support that I appreciate profoundly.

I also need to thank Dr. Yiling Hu for a level of support and kindness to which I cannot possibly do justice in written words. From the first day that I began in the lab, her selflessness, intelligence and energy have enabled and encouraged me to learn, work hard and progress. I will always appreciate what she has done for me as a teacher.

Equally, I want to thank Ranga Rankaduwa, not just as a friend and colleague, but also as someone who has repeatedly gone out of his way to provide counsel, always with utmost tact and efficacy. I also thank lab members Matthew MacDougall and Borbala Podor for challenging me to become a more careful thinker and for always being open to questions.

To Dr. Stefan Krueger, Annette Kolar and Dylan Quinn, I extend a massive thank-you for the provision of neuron cultures and the mCherry-GCaMP6f construct, and for always being available for advice and discussion.

I thank Alexander Goroshkov and Dr. Alexey Faustov for their technical assistance.

I also thank every member of the Fine lab for the environment they have helped cultivate and of which I have found myself lucky to be a part.

Lastly, I would like to thank my family, without whom none of this would be possible.

CHAPTER 1

Introduction

1.1 Neuronal Calcium Signalling

Calcium (Ca^{2+}) signalling is a ubiquitous and dynamic biochemical process in virtually all eukaryotic cells. In neurons, its role extends from basic homeostatic mechanisms to those that convert incoming synaptic information to persistent, activity-dependent changes in electrophysiological behaviour. In fact, one of the most intensely-studied aspects of Ca^{2+} signalling has to do with the flow of Ca^{2+} from the cytosol to the nucleoplasm, which is now known to trigger transcriptional responses necessary for adaptive changes in neuronal activity (Zhang et al., 2009). Moreover, this process can occur by means of numerous distinct types of Ca^{2+} elevation. Indeed, neurons are equipped with a remarkably diverse toolkit for the regulation of Ca^{2+} levels in various cellular domains, which can be harnessed to couple different incoming signals with specific downstream responses (Berridge et al., 2000).

A critical component of this dynamic involves the mechanisms that govern Ca^{2+} in the cytosol, maintaining tight control during resting states and allowing for robust increases during signalling.

1.1.1 Cytosolic calcium dynamics

A critical feature of Ca^{2+} handling in neurons is the maintenance of a steep concentration gradient across the plasma membrane and between the lumen of intracellular Ca^{2+} stores [i.e. the endoplasmic reticulum (ER)] and the cytosol. Typically, the cytosolic Ca^{2+}

concentration ($[Ca^{2+}]_i$) is held at approximately 10^{-7} M, 10,000-fold lower than the 10^{-3} M extracellular concentration (Simons, 1998). Maintaining this gradient requires the coordinated action of plasma membrane exchange pumps, cytosolic Ca^{2+} buffering proteins, and uptake into stores such as the ER and mitochondria (Brini et al., 2014).

1.1.1.1 Regulation of cytosolic calcium

Extrusion through the plasma membrane is a key mechanism of Ca^{2+} clearance in neurons, and is primarily attributed to two distinct membrane proteins: the sodium-calcium exchanger (NCX) and the plasma membrane Ca^{2+} ATPase (PMCA; Bano et al., 2005; Brini and Carafoli, 2010).

The NCX is found in three isoforms - NCX1-3 - that are expressed at different levels in various tissues but are all found in the brain (Blaustein and Lederer, 1999). It uses energy from the flow of sodium ions (Na^+) down their plasmalemmal electrochemical gradient into the cell to remove Ca^{2+} ions against their gradient to the extracellular space, with a ratio of three to one, respectively. By virtue of its low affinity for Ca^{2+} and rapid action, the NCX is critical in returning $[Ca^{2+}]_i$ to resting levels and preventing excitotoxicity following large elevations, such as those induced by depolarization (Blaustein and Golovina, 2001).

The plasma membrane Ca^{2+} ATPase (PMCA) similarly has different isoforms (PMCA1-4) that vary in their expression patterns but are all found in the brain (Niggli et al., 1982). Analyses of PMCA variants and knockouts have demonstrated that it contributes to both

basal Ca^{2+} regulation and clearance of signalling-induced Ca^{2+} elevations (Oceandy et al., 2007). In all, the combined actions of the NCX and PMCA are crucial for the precise maintenance of cytosolic Ca^{2+} levels in neurons.

Apart from extrusion, cytosolic Ca^{2+} is also controlled by uptake into intracellular stores. The sarco/endoplasmic reticulum ATPase (SERCA), particularly its SERCA2b and SERCA3 isoforms, is robustly expressed on the membrane of the ER in neurons (MacLennan et al., 1997). Through an ATP-dependent process, SERCA pumps remove cytosolic Ca^{2+} to the ER lumen during resting conditions and in response to large cytosolic elevations (Takeuchi et al., 2013; Verkhratsky and Peterson, 1998). This occurs in a manner that is sensitive to both cytosolic and luminal Ca^{2+} levels, as well as to signalling by interactions with proteins such as protein kinase A (PKA), which increases the rate of uptake.

Although SERCA-mediated uptake into the ER has been established as the predominant store-related mechanism for setting resting cytosolic Ca^{2+} in neurons, sequestration by other organelles, such as mitochondria, is also an important factor (Hajnoczky et al., 1999). In fact, the NCX is found on the outer mitochondrial membrane. Additionally, the more recent discovery of the ER's mitochondria-associated membrane (MAM) domains, where the ER and mitochondria are structurally and functionally tethered, furthers the notion that mitochondria contribute to Ca^{2+} handling in neurons (Raturi and Simmen, 2013). The mitochondrial Ca^{2+} uniporter (MCU) is a third mechanism of uptake into

mitochondria, and is dependent on cytosolic Ca^{2+} concentration and driven by the inner mitochondrial membrane potential (Kirichok et al., 2004).

Finally, regulation of Ca^{2+} can be in part carried out by the buffering effect of the wide range of Ca^{2+}-binding proteins present in the cytosol. Importantly, the function of many of these proteins is not restricted to simple chelation, as many of them have been identified as important components of Ca^{2+} signalling cascades. The best characterized example of this is calmodulin (CaM), which, upon Ca^{2+} binding, undergoes conformational changes that drive its many downstream interactions, among them binding to Ca^{2+}/CaM-dependent protein kinases (CaMKs) as part of synaptic plasticity-related transcription cascades (Chin and Means, 2000). Either as part of signalling cascades or purely as a buffering mechanism, the many cytosolic Ca^{2+}-binding proteins in neurons present yet another method of Ca^{2+} regulation.

The aggregate effect of the above-mentioned Ca^{2+} control mechanisms, and the maintenance of concentration gradients across the plasma and internal store membranes, is that neurons are endowed with the ability to generate different forms of Ca^{2+} elevation as triggers for, or parts of, their many signalling cascades.

1.1.1.2 Mechanisms of cytosolic calcium elevation

As mentioned, there are few neuronal processes that occur with absolutely no direct or indirect involvement of Ca^{2+}. In the context of neurotransmission specifically, increases

in cytosolic Ca^{2+} have an initiatory or modulatory role at virtually every step ranging from the presynaptic terminal to dendritic and somatic responses of the postsynaptic cell.

The arrival of an action potential at the synaptic terminal triggers the opening of plasma membrane-localized voltage-gated calcium channels (VGCCs) (Westenbroek et al., 1990). Of the different VGCC classes (L-, N-, P-, Q-, R- and T-), the N-, P/Q-, and R-forms - all of which are high voltage-gated and consist of an α_1 subunit that forms their pore and defines their physiological characteristics - are typically associated with influx at synaptic terminals (Hofmann et al., 1999). Specifically, their action provides the Ca^{2+} elevation necessary for vesicular docking and fusion and neurotransmitter release.

Advances in revealing the role of Ca^{2+} in the postsynaptic response to neurotransmitter binding have been made possible to a great extent by studies carried out in the dendritic spines of hippocampal neurons. Following synaptic activity, Ca^{2+} entry into spines may begin with influx through ionotropic glutamate receptors (Stuart and Sackmann, 1994). Specifically, following ligand binding, the flow of Na^+ and K^+ through α-amino-3-hydroxy-5-methyl-4-isoxazolepropionic acid receptors (AMPARs) causes magnesium ion (Mg^{2+}) to be removed from the pore of *N*-methyl-D-aspartate receptors (NMDARs), allowing Ca^{2+} to enter the spine through the NMDAR pore (Sabatini et al., 2002; Svoboda et al., 1997; Higley and Sabatini, 2012). Additionally, action potentials backpropagating from the soma can cause further depolarization and additional Ca^{2+} influx. Evidence for a direct AMPAR contribution to this influx is scarce. AMPARs that possess a GluR2 subunit, which is true in the majority of cases, are impermeable to Ca^{2+}

(Cull-Candy et al., 2006). Even in experiments involving GluR2-lacking AMPARs, the degree of Ca^{2+} influx through these receptors relative to the total synaptically evoked Ca^{2+} entry in the spine has been shown to be low (Nakagawa, 2010). The predominant mechanism of glutamatergic transmission-driven Ca^{2+} elevation at dendritic spines seems to involve AMPAR-dependent relief of NMDAR Mg^{2+} block and subsequent Ca^{2+} influx through NMDARs.

In addition to glutamate receptors, Ca^{2+} influx at dendritic spines can in part be driven by VGCCs (Miyakawa et al., 1992). Depolarization induced by ligand binding as well as by backpropagating action potentials can trigger the opening of VGCCs. Experimental evidence for the significance of this mechanism, however, has been mixed. For example, in response to backpropagating action potentials induced by somatic current injection, Ca^{2+} influx in the dendritic spines of CA1 pyramidal neurons was found to be mediated primarily by R-type VGCCs (Yasuda et al., 2003). In another study, EPSPs elicited by a stimulating electrode in the stratum radiatum triggered Ca^{2+} influx in CA1 and CA3 dendritic spines that were heavily dependent on release from the ER, and pharmacological inactivation of VGCCs yielded no effect (Emptage et al., 1999).

In the latter study, application of cyclopiazonic acid (CPA), which inactivates SERCA pumps and depletes intracellular Ca^{2+} stores (Soler et al., 1998), was found to cause a significant reduction in EPSP-induced Ca^{2+} elevation in the spine (Emptage et al., 1999). Further analysis indicated that the mechanism of store release was primarily attributed to ryanodine receptors (RyRs), which are known to contribute to calcium-induced calcium

release (CICR) - a regenerative process in which elevated cytosolic Ca^{2+} levels open RyRs, causing additional elevation, activation of neighbouring RyRs and propagation of a Ca^{2+} wave (Usachev et al., 1993). Consistent with this, RyR-mediated store release in dendritic spines of cortical neurons has been shown to serve an important function of inducing long-term enhancement of Ca^{2+} transients elicited by backpropagating action potentials, with potential implications in plasticity (Johenning et al., 2015). Similarly, CICR by RyRs in dendritic spines of hippocampal neurons has been shown to be necessary for long-term potentiation (LTP; Raymond and Redman, 2006).

RyR-mediated release is one of two mechanisms for store release, the other involving inositol 1,4,5-trisphosphate receptors (IP_3Rs). It has long been established that activation of Group 1 metabotropic glutamate receptors (mGluRs) and muscarinic acetylcholine receptors (AChRs) leads to phospholipase C (PLC) and IP_3 upregulation, which, along with free Ca^{2+}, triggers the opening of IP_3Rs (Simpson et al., 1995; Korkotian and Segal, 1998). In the dendritic spines of cerebellar Purkinje neurons, this mechanism is turned on by synaptic activity (Watanabe et al., 2006). Considering studies in which store depletion was not associated with a change in spine Ca^{2+} dynamics (Sabatini et al., 2000), however, it again seems that whether or not IP_3R-mediated Ca^{2+} release plays a role in dendritic spines is dependent on experimental conditions. In fact, given that the presence of both Ca^{2+} stores and VGCCs in dendritic spines has been demonstrated (Sharp et al., 1993), state- and cell type-dependent difference in their contribution are possible.

Beyond the spine, this combination of Ca^{2+} entry through the plasma membrane and release from stores is observed throughout the dendrite and soma. In response to excitatory postsynaptic potentials (EPSPs) and action potentials (including those backpropagating from the soma), L-type VGCCs located in the dendritic and somatic plasma membrane open to allow Ca^{2+} influx (Ahlijanian et al., 1990; Magee and Johnston, 1995; Simms and Zamponi, 2014). These are often termed Ca^{2+} *spikes* to differentiate them from the larger and slower Ca^{2+} *waves* elicited by store release (Henzi and MacDermott, 1992). Interestingly, it has been suggested that owing to their relatively slow activation kinetics, somatic L-type VGCCs may be most effectively activated by EPSP build-up rather than by action potentials (Mermelstein et al., 1999).

Either triggered by or independent of VGCC-mediated Ca^{2+} influx, release from the ER can also play a significant role in dendritic and somatic Ca^{2+} elevation (Berridge, 1998). Structurally, the ER network extends through the entirety of the dendritic arbor, soma and axon. RyRs and IP_3Rs are found throughout this network, with separate and overlapping expression patterns (Seymour-Laurent and Barish, 1995). Both are present in the somata and dendrites of hippocampal neurons, whereas only RyRs, of which the most abundant isoform is RyR3, have been detected in individual spines (Hakamata et al., 1992; Seymour-Laurent and Barish, 1995). Functionally, both receptor types are controlled by a complex interaction between cytosolic Ca^{2+}, luminal Ca^{2+}, and binding partners on both sides of the ER membrane (Kano et al., 1995; Lorenzon et al., 1995). Both RyRs and IP_3Rs are more likely to open when the ER is sufficiently filled and cytosolic Ca^{2+} levels are elevated. RyR-mediated Ca^{2+} release is modulated by a variety of cytosolic proteins,

among them CaM, calstabin and PKA, all of which contribute to the ability of the RyR complex to tune its responses to changes in Ca^{2+} levels (Zalk et al., 2007). The generation of IP_3R-mediated Ca^{2+} release is known to rely on the coincidence of Ca^{2+} elevation and build-up of IP_3, for instance by Group 1 mGluR or mAChR activity, as well as on cytosolic modulatory proteins (Barbara, 2002).

In the simplest sense, once activated, both RyRs and IP_3Rs release ER Ca^{2+} that can activate neighbouring receptors, setting off a regenerative wave capable of elevating cytosolic Ca^{2+} levels over extended areas. In reality, it has become increasingly clear that these two systems are capable of a multitude of distinct forms of Ca^{2+} release, ranging from transient, local increases to global Ca^{2+} waves that cover the majority of the neuron (Brini et al., 2013).

For instance, spontaneous RyR-mediated events in hippocampal CA1 pyramidal neurons, termed "sparks," have been observed in dendrites, in which Ca^{2+} is elevated transiently with a time-to-decay to half-peak amplitude of approximately 67 ms, and spreads over a dendritic region of just a few μm (Miyazaki and Ross, 2013). These sparks have been shown to be independent of IP_3R contribution. Release from the ER that is IP_3R-dependent, lasts slightly longer (time-to-half peak of up to 200 ms) and is capable of covering a larger stretch of the dendrite (termed "puff") has also been described (Miyazaki and Ross, 2013).

Much of the information regarding *global* RyR-mediated Ca^{2+} waves has come via studies employing caffeine, a potent agonist of the RyR receptor that increases its sensitivity such that resting cytosolic Ca^{2+} levels may become stimulatory (Shmigol et al., 1994). In many cell types, including dorsal root ganglion (DRG), CA1 and CA3 hippocampal neurons, bath application of caffeine induces a wave that spreads bidirectionally throughout the soma and dendritic body, and is preventable by the inactivation of RyRs (Shmigol et al., 1994). Similarly, activation of metabotropic receptors in hippocampal neurons can induce global IP_3R-mediated waves. For example, in response to muscarine and carbachol, muscarinic acetylcholine receptor (mAChR) agonists, calcium waves that begin in the proximal apical dendrite and invade the soma can be elicited (Power and Sah, 2002).

The mechanisms described thus far are capable of acting independently. For instance, action potential- and L-type VGCC-dependent Ca^{2+} spikes measured in the somata of CA3 neurons have been observed to be unchanged by the inhibition of RyR- and IP_3R-mediated store release (Raymond and Redman, 2006). Similarly, IP_3R-mediated waves have been shown to be unaffected by the inactivation of RyRs. Whether RyRs are capable of propagating global waves with simultaneous pharmacological block of IP_3R-mediated release, however, has not been directly addressed.

Nevertheless, it is important to emphasize that a great amount of experimental evidence has demonstrated the tendency of these systems to act cooperatively as well. For example, preincubation of hippocampal pyramidal neurons with caffeine (and thus

sensitization of RyRs) during action potential- and L-type VGCC-dependent Ca^{2+} transients leads to a potentiation of the Ca^{2+} response (Sandler and Barbara, 1999). Additionally, it has been suggested that the probability that an IP_3R-mediated wave will propagate successfully to the soma can be increased by the presence of backpropagating action potentials (Watanabe et al., 2006). It has also been shown that action potentials in CA1 pyramidal neurons can be potentiated by RyR-mediated CICR (Sandler and Barbara, 2002). Finally, cytosolic Ca^{2+} spikes in response to action potential trains can be potentiated with simultaneous muscarinic activation (Power and Sah, 2002)

1.1.2 Functions of cytosolic calcium signaling

The functional consequences of elevated Ca^{2+} levels in the cytosol are numerous. Among them, however, one of the most intensely-studied contexts involves activity-dependent changes in neuronal behaviour.

In particular, the study of LTP in hippocampal neurons has yielded the view that different forms of LTP – e.g. early LTP (E-LTP), which is transient in duration, and late LTP (L-LTP), which lasts much longer and may be permanent - rely on distinct mechanisms that employ different forms of Ca^{2+} signalling (Raymond and Redman, 2006). Ca^{2+} elevation in dendritic spines via NMDARs and RyR-mediated CICR has been shown to be necessary for the induction of E-LTP, which is consistent with the notion that this form of LTP is associated with post-translational modification of synaptic proteins (Emptage et al., 1999). On the other hand, induction of the durable L-LTP is suggested to require somatic VGCCs (Raymond and Redman, 2006). This is again in line with the

understanding that L-LTP is transcription-dependent, and that elevations in *nuclear* calcium are required for the necessary transcriptional events (Hardingham et al., 1997).

Because of this, a significant amount of emphasis is placed on studying not only cytosolic Ca^{2+}, but also the dynamics of Ca^{2+} signalling between the cytosol and nucleus. Given the growing body of knowledge on the necessity of nuclear Ca^{2+} for transcription-dependent LTP (Limback-Stokin et al., 2004), and that Ca^{2+} signalling in the nucleus is also responsible for cellular functions apart from LTP (Zhang et al., 2007), a key objective is to characterize the different forms of Ca^{2+} entry into the nucleus as the foundation for better understanding of how these distinct mechanisms lend themselves to various forms of activity-dependent plasticity and other neuronal processes.

1.2 Nuclear Calcium Signaling in Neurons

One of the first and fundamental observations about nuclear calcium transients in neurons was that they displayed different characteristics compared to those in the cytosol (Bengtson and Bading, 2012). Advancements in Ca^{2+} imaging have allowed for better understanding of the mechanisms by which nuclear Ca^{2+} is elevated and cleared and have begun to uncover the functional consequences of Ca^{2+} increases in the nucleus. Still, there exists significant variability in experimental findings, ranging from those showing nuclear Ca^{2+} signals that are generated strictly by diffusion from the cytosol to those that point to release directly from the lumen (perinuclear space) of the nuclear envelope (NE). What is emerging as the likely reality is that each of these scenarios is important under specific circumstances, and this may in fact be one means by which neurons link specific

genomic responses (or lack thereof) to distinct incoming signals (Hagenston and Bading, 2011).

1.2.1 Features of the nuclear envelope

Nuclear pore complexes (NPCs) perforate the NE and allow for ion and macromolecule exchange between the nucleoplasm and cytoplasm via a central channel with an inner diameter of approximately 40 nm, which is expected to render them freely permeable to Ca^{2+} (Beck et al., 2004). Surprisingly, experimental evidence has presented a slightly less straightforward picture. Studies on isolated nuclei have proposed that the NPC can exist in a closed state, and in separate experiments, that the Ca^{2+} load of the NE can influence NPC conductance as part of a state-dependent gating mechanism (Lui et al., 1998). In the former case, it is possible that the findings were the result of unphysiological NPC behaviour induced by the experimental protocol. Whether or not NPC conductance is sensitive to NE Ca^{2+} levels remains to be clarified. What is clear, however, is that NPCs present a simple diffusion path for Ca^{2+} flowing from the cytosol to the nucleoplasm, and that restricted diffusion creates differences in the characteristics of nuclear and cytosolic Ca^{2+} elevations (Eder and Bading 2007; further detailed in Section 1.2.2).

Apart from the NPCs' function as conduits for Ca^{2+} flow between the cytosol and nucleus, there is evidence to suggest that the NE is itself able to release Ca^{2+} directly into the nucleoplasm. The NE is a double membrane with lumenal continuity with the ER (Gerace and Burke, 1988). This, along with SERCA pumps located on its outer membrane, allows the NE to sequester Ca^{2+} and act as a Ca^{2+} store. Nevertheless, the

conditions under which direct release from the NE contributes to nuclear Ca^{2+} elevation have been difficult to confirm experimentally, and are further described in the following section.

1.2.2 Mechanisms of nuclear calcium elevation and clearance

The best-characterized mechanism of nuclear Ca^{2+} influx involves the diffusion of Ca^{2+} from the cytosol. It has been established that there is a uniform distribution of Ca^{2+} between the cytosol and nucleus, with no concentration gradient (O'Malley, 1994). Because of this, elevations in cytosolic Ca^{2+} can readily lead to rises in the nucleus. A key example of this involves Ca^{2+} spikes induced by the activation of somatic L-type VGCCs by EPSPs or action potentials, in which membrane depolarization causes opening of somatic VGCCs and flow of Ca^{2+} into the cytosol, where it can invade the nucleus (Bengtson et al., 2010). In these scenarios, relative to cytosolic elevations, nuclear Ca^{2+} transients are smaller in amplitude, slower to reach their peak concentration and slower to decay as a result of the restricted diffusion path posed by NPCs (Eder and Bading, 2007).

The termination of these nuclear Ca^{2+} spikes is primarily attributed to diffusion back out through NPCs (Bootman et al., 2007). Indeed, the area around the nucleus has been shown to be rich in ER with high expression of SERCA pumps, which allow it to act as a sink for nuclear Ca^{2+}. Additional evidence for the presence of NCX pumps on the inner NE membrane has also been found (Ledeen and Wu, 2007), but the details of how they may contribute to nuclear Ca^{2+} clearance is not yet clear. Finally, as is the case in the

cytosol, nuclear Ca^{2+} can in part be buffered by nuclear-localized Ca^{2+}-binding proteins such as parvalbumin (Mauceri et al., 2015).

In similar fashion, Ca^{2+} *waves* that are sufficiently robust to propagate through the soma can invade the nucleus. For example, IP_3R-dependent waves initiated by bath application of muscarine or carbachol to hippocampal neurons generate nuclear Ca^{2+} elevations (Power and Sah, 2002), and RyR-mediated waves induced by caffeine can readily reach the nucleus in embryonic mouse telencephalic neurons (Tsai and Barish, 1995). As in the case of Ca^{2+} spikes, Ca^{2+} waves have been shown to evoke nuclear responses that are smaller in amplitude and slower than their cytosolic counterparts.

In summary, by virtue of the permeability of nuclear pores, the mechanisms of cytosolic Ca^{2+} events discussed in Section 1, particularly those that lead to *somatic* Ca^{2+} elevation, are all capable of generating nuclear Ca^{2+} influx. A much less clear mechanism, and a heavily investigated topic, involves the possibility of direct Ca^{2+} release from the NE to the nucleoplasm.

1.2.3 Calcium release from the nuclear envelope

Much of the evidence for direct release mechanisms from the perinuclear space of the NE to the nucleoplasm have come in the form of electrophysiological study of isolated nuclei. Patch-clamp recordings of isolated nuclei from Purkinje and granule neurons indicated the presence of IP_3-activated channels specifically localized on the inner NE membrane (Marchenko et al., 2005). This is in line with similar experimental approaches in non-neuronal cells showing NE-localized channel activity in response to IP_3 (Wagner

and Yule, 2011). In isolated nuclei of CA1 pyramidal neurons, evidence for inner NE-localized IP_3Rs has been found, while in dentate gyrus granule cells, RyRs have been suggested to exist on the outer NE (Fedorencko and Marchenko, 2014). It is also noteworthy that nuclei have been shown to possess the molecular machinery required for IP_3 production. For example, glutamate application to HEK cells and neurons expressing mGluRs on their nuclear membranes can elicit nuclear Ca^{2+} elevations and upregulation of nuclear IP_3 (Kumar et al., 2008; O'Malley et al., 2003).

Despite these lines of evidence, unambiguous demonstrations of Ca^{2+} release from the perinuclear space in intact neurons are lacking. For instance, a commonly raised question is whether nuclear Ca^{2+} signals can occur in the absence of cytosolic Ca^{2+} elevation, and clear evidence for this in neurons has been elusive.

Apart from the possibility of autonomous nuclear Ca^{2+} signals, it has been equally difficult to determine whether release from the NE simply contributes to nuclear Ca^{2+} elevations, such that Ca^{2+} influx from the cytosol is augmented by release from the NE. For instance, nuclear Ca^{2+} spikes evoked by bicuculline [a competitive antagonist of γ-Aminobutyric acid (GABA) receptors] were shown to be reduced when CPA was used to deplete stores (Hardingham et al., 2001). Because cytosolic Ca^{2+} levels were not simultaneously monitored, however, it is not possible to determine whether the reduced nuclear signals were driven by a disruption of NE release mechanisms, or simply a secondary effect of reduced Ca^{2+} transient amplitudes in the cytosol. Contrastingly, in a study on the nuclear Ca^{2+} signal associated with L-LTP-inducing high frequency

stimulation (HFS) and θ-burst stimulation (TBS), it was found that store depletion with CPA did not lead to any changes in the nuclear response (Bengtson et al., 2010).

Thus, there still exists a fundamental need to characterize different patterns of Ca^{2+} elevation in the cytosol and nucleus, and to determine whether or not release from the NE is an important component of these dynamics. In this respect, advancements in Ca^{2+} sensors have provided more sensitive and precise means of measuring Ca^{2+} in both compartments and have allowed more sophisticated experiments to be performed.

1.3 Imaging Nuclear Calcium Signals

Until recently, information regarding nuclear Ca^{2+} dynamics in neurons came largely from experiments using synthetic, small molecule Ca^{2+} indicators. While these studies led to critical discoveries regarding the characteristics and functions of nuclear Ca^{2+}, their dependence on the differential aggregation of dye in the nucleus vs. the cytosol for defining this boundary may have rendered them susceptible to misinterpretation of Ca^{2+} signals in certain cases. The recent emergence of genetically-encoded Ca^{2+} indicators (GECIs) provides an effective means of targeting Ca^{2+} sensors to the nucleus, allowing for unambiguous reporting of nuclear signals. Among the recently-developed GECIs, those of the GCaMP family have received particular attention on the basis of their robust fluorescence response and relatively fast on- and off-kinetics (Podor et al., 2015).

GCaMPs consist of a circularly permuted enhanced green fluorescent protein (EGFP) flanked on either side by CaM and the CaM-binding peptide, M13 (Nakai et al., 2001).

Ca^{2+} binding induces CaM/M13 interactions that result in conformational changes in the EGFP, leading to increased fluorescence.

There have already been recent reports of nuclear-targeted versions of GCaMPs. Work by Bengtson et al. (2010), previously discussed in the context of nuclear Ca^{2+} response to HFS and TBS, presented the first case of a nuclear-targeted GCaMP, in particular, GCaMP2. Subsequently, Ahrens et al. (2013) and Vladimirov et al. (2014) have developed nuclear-localized versions of GCaMP5 and GCaMP6, respectively, to carry out live, whole-brain imaging of zebrafish during visual tasks. Similarly, work by Kim et al. (2014) has led to the development of a nuclear-localized version of GCaMP3 for applications in brain-wide imaging of zebrafish.

Recently, we developed the first nuclear-localized version of GCaMP7, termed GCaMP7-NLS (unpublished data). Our interest in GCaMP7 in particular came from experiments performed in our lab showing that compared with other GECIs, it shows the most robust fractional change in response to Ca^{2+} elevations, has among the fastest kinetics and is sufficiently sensitive to reliably respond to individual action potentials (Podor et al., 2015).

1.4 Objectives

In the context of what has been described thus far regarding the need for characterization of cytosolic/nuclear Ca^{2+} dynamics, clarification of how and under what circumstances direct release from the NE may play a role in such dynamics, and the use of targeted Ca^{2+}

indicators for the visualization of Ca^{2+} transients in these compartments, this project consisted of the following objectives:

1. Characterize the fluorescence response properties of our recently developed GCaMP7-NLS sensor to confirm that it maintains the desirable features of cytosolic GCaMP7.
2. Perform simultaneous imaging of cytosolic and nuclear Ca^{2+} dynamics in dissociated hippocampal neurons to describe the differences in Ca^{2+} transient amplitude and kinetics associated with each compartment during spontaneous Ca^{2+} spike activity.
3. Carry out pharmacological manipulation of intracellular Ca^{2+} store uptake and release mechanisms and look for effects on the nuclear/cytosolic relationship to determine whether there are indications of direct Ca^{2+} release from the perinuclear space in the observed nuclear Ca^{2+} spikes.
4. Induce RyR-mediated Ca^{2+} waves and determine whether inactivation of IP_3Rs affects the ability of RyR-mediated waves to spread to the nucleus.

CHAPTER 2

Methods

2.1 Preparation of Dissociated Hippocampal Neuron Cultures

Dissociated hippocampal cells were prepared by and obtained from Annette Kolar, member of the Krueger lab (Department of Physiology and Biophysics, Dalhousie University, Halifax, NS). Preparation of the cultures began with a 1-hour treatment of German Glass No. 1 coverslips in 1 mM potassium chloride (KCl) followed by a wash with water and sterilization with 95% ethanol (EtOH) and flaming. Coverslips were then incubated in 0.05% (w/v) Poly-L-lysine (PLL; Peptides International) in 35 mm dishes overnight, followed by a wash with sterilized water and 2-hour or overnight incubation in 5% (v/v) fetal calf serum (FCS) at 37°C.

E18-19 rats were sacrificed by CO_2 inhalation and embryos were removed from uteri. Brains were removed and hippocampi were dissected out. The hippocampi from 6 brains were incubated in 0.03% trypsin (Sigma#T9935; essentially salt-free, lyophilized powder) for 12-15 minutes at 37°C. They were then washed four times with 1X Earle's Balanced Salt Solution (EBSS; calcium chloride-, magnesium sulphate- and phenol red-free; Gibco #14155-063), and triturated 15-20 times with a glass Pasteur pipette in 3 mL 1X EBSS.

Finally, hippocampal cells were diluted in Neurobasal Medium (Gigbco #21103-049) with 5% serum, plated at a density of 20,000-40,000 cells/mL and incubated at 37°C and

5% CO_2 for 2-3 hours, after which the medium was replaced with serum-free Neurobasal Medium and cells were returned to an incubator (37°C and 5% CO_2) until use.

2.2 Genetically Encoded Calcium Indicators (GECIs) and Calcium Phosphate Transfection

Cytosolic Ca^{2+} signals were measured by GCaMP6f (Chen et al., 2013) tagged with mCherry - mCherry-GCaMP6f. For visualization of nuclear signals, GCaMP7 (Ohkura et al., 2012) with three copies of a nuclear localization sequence (NLS) at its C-terminus - GCaMP7-NLS – was used. The NLS was obtained as part of a blue fluorescent protein plasmid (pEBFP2-Nuc; Addgene plasmid #14893).

DNA constructs for both sensors were introduced into dissociated hippocampal cells by calcium phosphate transfection. Cells were transfected at 11-13 days in vitro (DIV), beginning with the transfer of coverslips to a transfection medium consisting of Minimum Essential Medium (MEM; Life Technologies) with 30 mM HEPES (Sigma #7365-45-9), 1% (v/v) GlutaMAX (Life Technologies) and 2% (v/v) B-27 (Life Technologies). A transfection solution was made by combining the mCherry-GCaMP6f (2 µg/µl) and GCaMP7-NLS (2 µg/µl) DNA constructs (each totalling to 5-13.33% of the mixture), 2 M $CaCl_2$ (10%), and double-distilled H_20 (ddH_20), and adding them in 10% increments to an equal volume of HEPES-buffered saline (HEBS; 274 mM NaCl, 10 mM KCl, 1.4 mM Na_2HPO_4, 15 mM D-Glucose, 42 mM HEPES and ddH_20). The mixture was allowed to sit for 15-20 minutes, after which it was added to the transfection medium containing the coverslips in a drop-wise fashion. Cells were incubated with the

transfection mixture for 3-5 hours, washed with Hanks' Balanced Salts Solution (HBSS; 144 mM NaCl, 3 mM KCl, 2 mM $MgCl_2$, 10 mM HEPES and ddH_20) solution and returned to original media. Experiments were performed 24-48 hours post-transfection (i.e. at 12-14 DIV).

2.3 Experimental Protocol

2.3.1 Confirmation of cytosolic and nuclear calcium sensor localization

mCherry-GCaMP6f was used as the cytosolic Ca^{2+} sensor so that prior to experiments, its red, mCherry tag could be used to confirm that it was restricted to the cytosol and that (green) GCaMP7 expression was restricted to the nucleus (Figure 2.1). For this purpose, cells were imaged using a Nikon inverted fluorescence microscope with a 100 W xenon arc lamp. mCherry was visualized with a triple band filter (excitation: 395-410, 490-505, and 560-580 BP; dichroic mirror: 445-480, 510-555, and 590-665 BP; emission: 450-470, 515-545, 600-650 BP), and GCaMP fluorescence was visualized using a High Q filter with 480/40 excitation BP, 505 LP dichroic mirror and 535/50 emission BP. All images were captured by ToupView software (ToupTek Photonics).

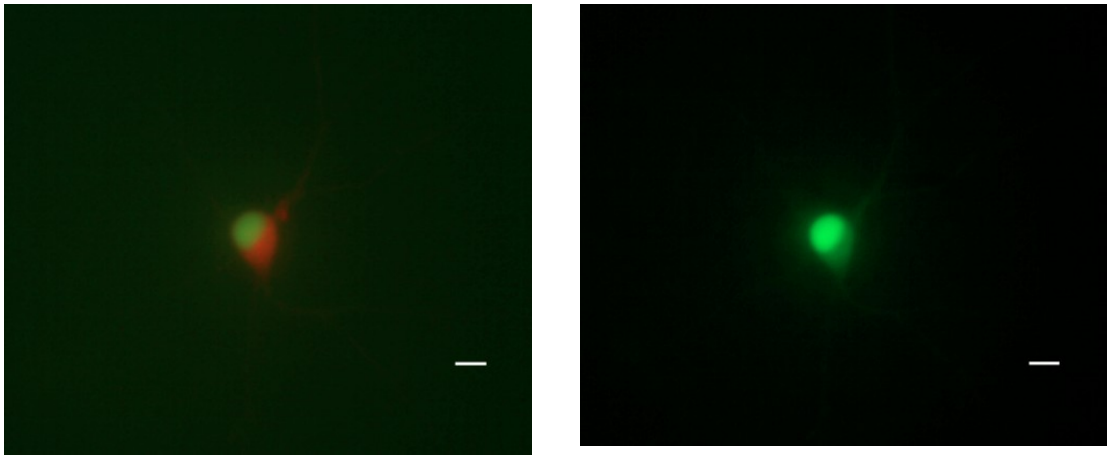

Figure 2.1. *Example of an mCherry-GCaMP6f- and GCaMP7-NLS-expressing hippocampal neuron.* Left: a transfected cell viewed with a triple band filter demonstrating restriction of mCherry-GCaMP6f expression to the cytosol and nuclear-localization of GCaMP7-NLS. Right: the same cell viewed with a blue excitation filter showing GCaMP6f (cytosolic) and GCaMP7-NLS (nuclear) fluorescence. Scale bars = 10 μm.

2.3.2 Calcium Imaging Experiments

A coverslip with dissociated hippocampal neurons expressing mCherry-GCaMP6f and GCaMP7-NLS was removed from its medium and placed in a chamber with 500-750 µl imaging buffer (124mM NaCl, 3mM KCl, 2mM $CaCl_2$, 1mM $MgCl_2$, 10mM HEPES, 5mM D-Glucose and ddH_20) and returned to the incubator for 10 minutes. After removal from the incubator, the chamber was positioned on the stage of a Zeiss IM 35 inverted microscope with a Thorlabs blue (470 nm) mounted high-power LED and 100X oil immersion objective (1.25 numerical aperture). GCaMP fluorescence was visualized using a filter with 450-490 excitation BP, 510 LP dichroic mirror and 515-565 emission BP. Recordings were made at 60 frames/second using a Hamamatsu EM-CCD camera and collected and analyzed using HCImage Live software (Hamamatsu Corporation; Figure 2.2). Specifically, a region of interest (ROI) positioned on the extranuclear somatic region yielded mean grey value measurements corresponding to cytosolic fluorescence, and a nuclear ROI allowed for measurement of mean grey values corresponding to nuclear fluorescence.

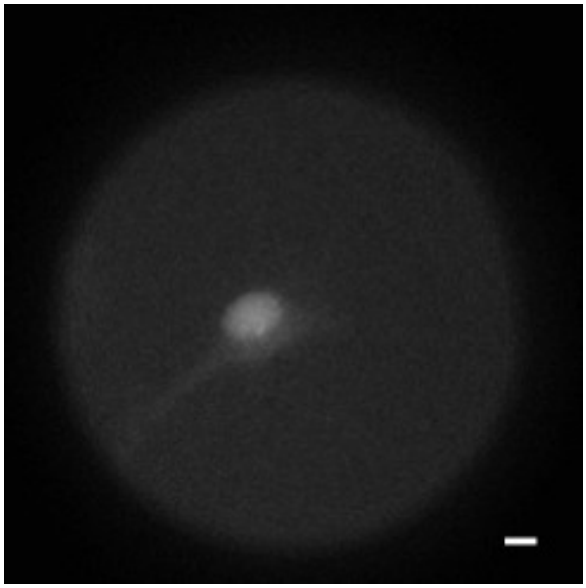

Figure 2.2. *Example of an mCherry-GCaMP6f- and GCaMP7-NLS-expressing hippocampal neuron viewed with Hamamatsu EM-CCD camera.* A hippocampal neuron showing basal nuclear (GCaMP7-NLS) and cytosolic (mCherry-GCaMP6f) fluorescence. Nuclear fluorescence was typically higher than cytosolic fluorescence at rest, possibly owing to differential expression of each sensor or the influence of the different biochemical environments of the nucleus and cytosol on each sensor. Scale bar = 10 μm.

In experiments involving induced depolarization, KCl was added to the imaging buffer directly at a final concentration of 40-60 mM.

Amplitudes of Ca^{2+} transients were measured as the change in fluorescence relative to baseline ($\Delta F/F$), and rise times were defined as time from baseline to peak fluorescence.

Experiments in which cells were treated with CPA (30 μM final concentration), ryanodine (25-30 μM final concentration) or xestospongin C (Xec; 5 μM final concentration) began as described above to allow for measurement of pre-drug nuclear/cytosolic fractional change associated with Ca^{2+} spikes. In particular, the nuclear fractional change was expressed as percentage of cytosolic fractional change. This method of analysis was used in order to specifically address the possibility of Ca^{2+} release from the perinuclear space: if the post-drug nuclear fractional change (expressed as percentage of cytosolic fractional change) was significantly different, it would suggest that release from the NE had been disrupted by the manipulation.

Once pre-drug fractional changes had been measured, drugs from a stock solution (dissolved in DMSO) were directly pipetted into the bath solution, with the final DMSO concentration remaining at 0.1% for CPA and ryanodine experiments and 0.5% for XeC experiments. Cells were then incubated at 37°C and 5% CO_2 for 20 minutes (CPA and ryanodine) or 10 minutes (XeC), and returned to the imaging setup for post-drug measurement of nuclear/cytosolic fractional change associated with Ca^{2+} spikes. For

control trials, DMSO (0.1% final concentration and duration matching the corresponding experimental protocol) was pipetted directly into the bath solution.

To assess the efficacy of CPA and ryanodine, a stock solution of caffeine (dissolved in water) was pipetted directly into the imaging buffer for a final concentration of 5 mM after incubation with each drug to confirm that the store-dependent Ca^{2+} elevation normally elicited by caffeine (Shmigol et al., 1994) was abolished.

Finally, in experiments specifically aimed at characterizing caffeine-induced Ca^{2+} waves, control responses in the cytosol and nucleus were measured by bath application 5 mM caffeine. To test caffeine-induced responses in the presence of XeC, cells were first incubated in 5 μM XeC for 10 minutes prior to the start of imaging, after which caffeine was applied as described. All imaging was carried out at room temperature.

2.4 Statistical Analysis

Where indicated, two-tailed t-tests (performed using Microsoft Excel 2016) were used to assess significance. T-tests were unpaired in all cases except when comparing nuclear fractional change (expressed as percentage of cytosolic fractional change) for single spikes vs. spike build-ups, in which a paired t-test was used. All values are reported as mean ± standard error of the mean.

CHAPTER 3

Results

3.1: Characterization of GCaMP7-NLS and mCherry-GCaMP6f maximum fluorescence response

To characterize the fractional change associated with our recently developed GCaMP7-NLS sensor, we expressed the indicator in dissociated hippocampal neuron cultures via calcium phosphate transfection, and used bath application of a saturating concentration of KCl (40-60mM) to induce depolarization-dependent Ca^{2+} influx. We also assessed the response of the cytosolic mCherry-GCaMP6f sensor both as a means of comparison and because our subsequent experiments involved this indicator as well.

We found that GCaMP7-NLS showed a maximum fractional change ($\Delta F/F$) of 1682.4 ± 291% (n=7), while the same stimulus led to a 1396.2 ± 103% (n=7) change in mCherry-GCaMP6f fluorescence (Figure 3.1).

Our GCaMP7-NLS measurement is relatively consistent with a recent report from our lab showing that in response to eight action potentials at 100 Hz, cytosolic GCaMP7 expressed in hippocampal slices was associated with a maximum response of 1351 ± 147% (Podor et al., 2015). This indicated that targeting GCaMP7 to the nucleus did not jeopardize its maximum fluorescence response properties, and that GCaMP7-NLS signals were thus sufficiently robust for use in our subsequent experiments. Similarly, the response measured for GCaMP6f showed that it too produced a strong signal.

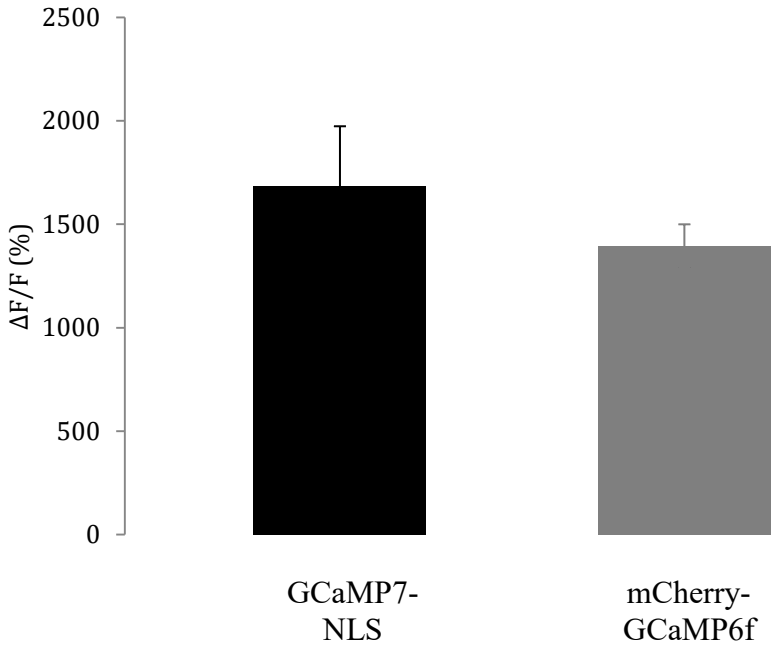

Figure 3.1. *Maximum fractional changes measured in the cytosol and nucleus.* Depolarization by application of 40-60 mM KCl induced maximum fluorescence responses by GCaMP7-NLS and mCherry-GCaMP6f of 1682.4 ± 291% and 1396.2 ± 103%, respectively (n=7 for each).

3.2: Simultaneous imaging of cytosolic and nuclear calcium dynamics

3.2.1 Basic patterns in cytosolic and nuclear calcium transients

In our first imaging paradigm, we measured spontaneous cytosolic and nuclear Ca^{2+} spike activity simultaneously using mCherry-GCaMP6f- and GCaMP7-NLS-co-expressing cells. Figure 3.2 shows a representative trace of the typical Ca^{2+} dynamics we measured in the cytosolic (grey trace) and nuclear (black trace) compartments. We found that every cytosolic transient was followed by Ca^{2+} elevation in the nucleus, with key differences. Nuclear transients had a smaller amplitude, slower rise and slower decay, as can be seen in the overlay of the cytosolic and nuclear Ca^{2+} elevations from a single spike in Figure 3.3.

To quantify this, we measured the fractional change and kinetics associated with the smallest observable transient for each cell that was imaged. To clarify, because we dealt with spontaneous activity, we typically observed a variety of Ca^{2+} events in any one imaging experiment, ranging from single spikes to elevations made of multiple spikes that built up on one another. In order to remain consistent when analysing these dynamics, we measured the nuclear and cytosolic signals associated with the smallest (i.e. single) spikes from each trace. In fact, the relatively low variability associated with our fractional change and kinetic data displayed in Figures 3.4 and 3.5 suggests that, in the majority of cases, we were measuring the same or similar physiological event. Without simultaneous recording of electrical activity, we were limited to hypothesizing about the mechanism driving the observed spikes. However, given the modest amplitude and fast rise times associated with the smallest spikes, it is likely that our observations

were of somatic VGCC-initiated events triggered by single or small numbers of action potentials, especially when comparing with prior studies demonstrating nuclear-targeted GCaMP signals in response to action potentials (Bengtson et al., 2010).

The mean ΔF/F measured for the smallest spike from 11 cells was 12.3 ± 1.2% in the cytosol and 4.21 ± 0.46% in the nucleus (Figure 3.4). Statistical comparison of the two showed that they were significantly different ($p<0.05$), indicating that we were able to distinguish between cytosolic and nuclear transients successfully with our setup. Rise times for cytosolic and nuclear spikes were 125 ± 9.2 ms and 178.8 ± 11.0 ms, respectively (Figure 3.5), and their difference was again statistically significant ($p<0.05$).

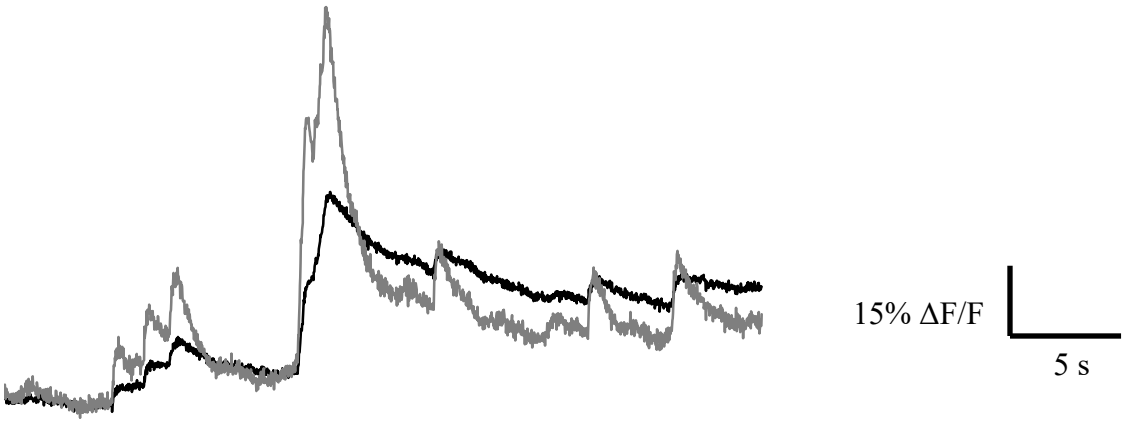

Figure 3.2. *Representative traces of cytosolic and nuclear calcium spikes.* Nuclear (black) events typically had slower rise times, slower decays and smaller amplitudes than their cytosolic (grey) counterparts. Traces have been normalized to baseline.

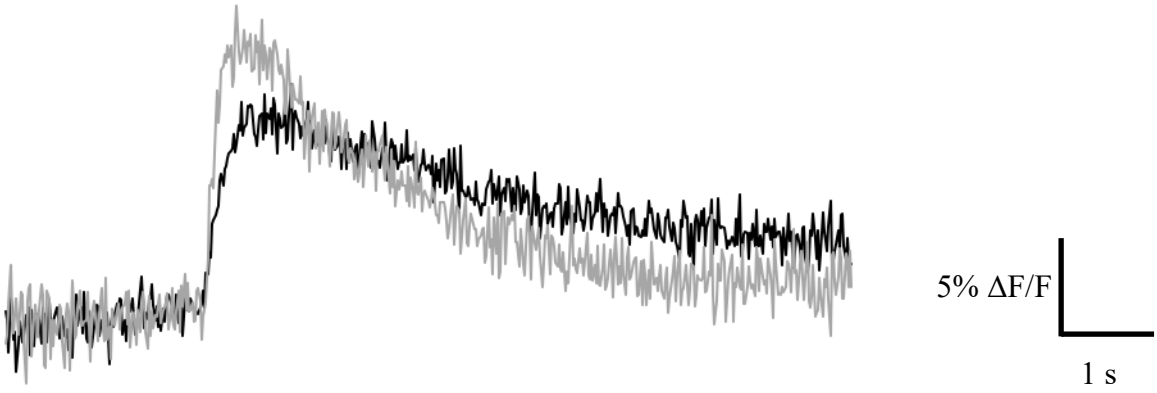

Figure 3.3. *Cytosolic and nuclear Ca^{2+} signal fractional change and kinetics associated with a single spike*. Cytosolic and nuclear traces for a single spike emphasize the trends shown in Figure 3.2: nuclear (black) spikes were slower to reach their peak, slower to decay, and were smaller in amplitude than cytosolic (grey) spikes. Traces have been normalized to baseline.

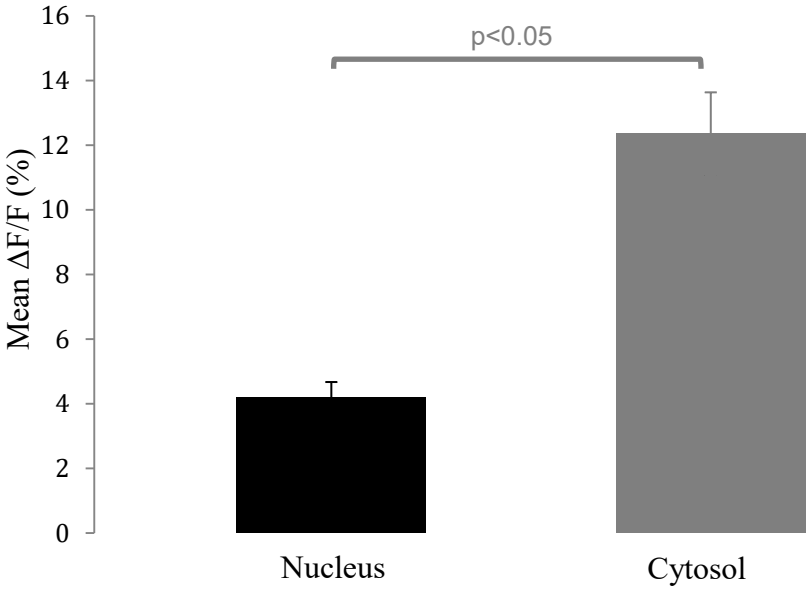

Figure 3.4. *Mean fractional change for single nuclear and cytosolic Ca^{2+} spikes*. The average fractional change for a single spike in the nucleus was significantly smaller compared to that of the cytosol (n=11; $p<0.05$).

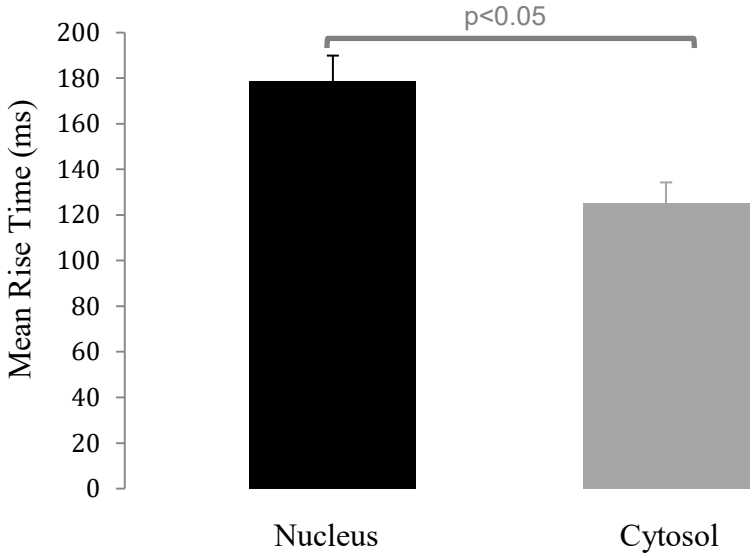

Figure 3.5. *Mean rise times of single nuclear and cytosolic Ca^{2+} spikes*. Single nuclear spikes were associated with significantly longer rise times compared to those in the cytosol (n=11; $p<0.05$).

In some cases, we found that we were unable to fit exponential functions for the analysis of *decay* kinetics. This may be due to limitations in our imaging setup, in that the signal-to-noise ratio associated with a single, modest Ca^{2+} transient leads to decays that do not display the properties necessary to be properly fit with an exponential function. Because of this, we limited our analysis of decays to a qualitative comparison. Figures 3.2 and 3.3 provide examples of the prolonged decay associated with the nuclear Ca^{2+} dynamics we measured compared to those in the cytosol, consistent with the understanding of Ca^{2+} clearance in these compartments, a key aspect of which is the kinetic barrier posed by NPCs for Ca^{2+} diffusing back out of the nucleus (Brini et al., 2014).

This points to an important feature of nuclear Ca^{2+} transients, in that their slower decay rate facilitates more robust build-up in response to rapid trains of spikes relative to cytosolic transients. This property is explored in more detail in Section 3.2.3. To demonstrate that this observation was not associated with a pathological process, we have included representative traces in Figure 3.6 that show cytosolic and nuclear build-ups that rapidly recover to baseline in the absence of further transients.

These preliminary findings set the basis for subsequent experiments aimed at further analyses of the relationship between cytosolic and nuclear Ca^{2+} spikes.

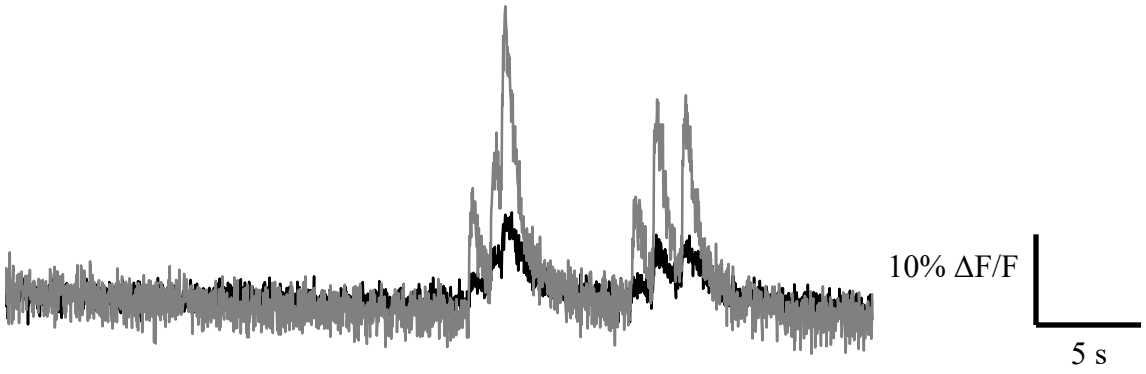

Figure 3.6. *Cytosolic and nuclear Ca^{2+} spike traces showing rapid recovery to baseline from build-up*. Build-up following a train of Ca^{2+} spikes recovered to baseline in the absence of further transients, indicating that the process was driven by the frequency of the spikes and inherent cytosolic and nuclear decay rates, and is not attributed to declining cell health.

3.2.2 The nuclear/cytosolic relationship remained stable at the level of single spikes in any one cell

For the duration of imaging in any one cell, we found that the ratio between nuclear and cytosolic Ca^{2+} spike amplitudes, or more intuitively expressed as nuclear Ca^{2+} spike fractional change as percentage of cytosolic Ca^{2+} spike fractional change, remained relatively stable at the level of single spikes. In Figure 3.7, three representative spikes per trace were chosen at random and labeled with this value. Figure 3.8 shows this trend for 10 cells.

Having established a means of quantifying the nuclear/cytosolic relationship, we applied this method in two subsequent series of analyses. First, we sought to compare this ratio when measured at the level of single spikes relative to when measured for a train of rapid, consecutive spikes (Section 3.2.3). Second, we aimed to address possible underlying mechanisms for these Ca^{2+} elevations. It was possible that the observed spikes were driven exclusively by diffusion of Ca^{2+} through the nuclear pores. Alternatively, direct release of Ca^{2+} from the perinuclear space may have contributed to the total nuclear fractional change. We therefore carried out experiments in which store release and uptake mechanisms were pharmacologically altered to attempt to address each of these possibilities (Section 3.3).

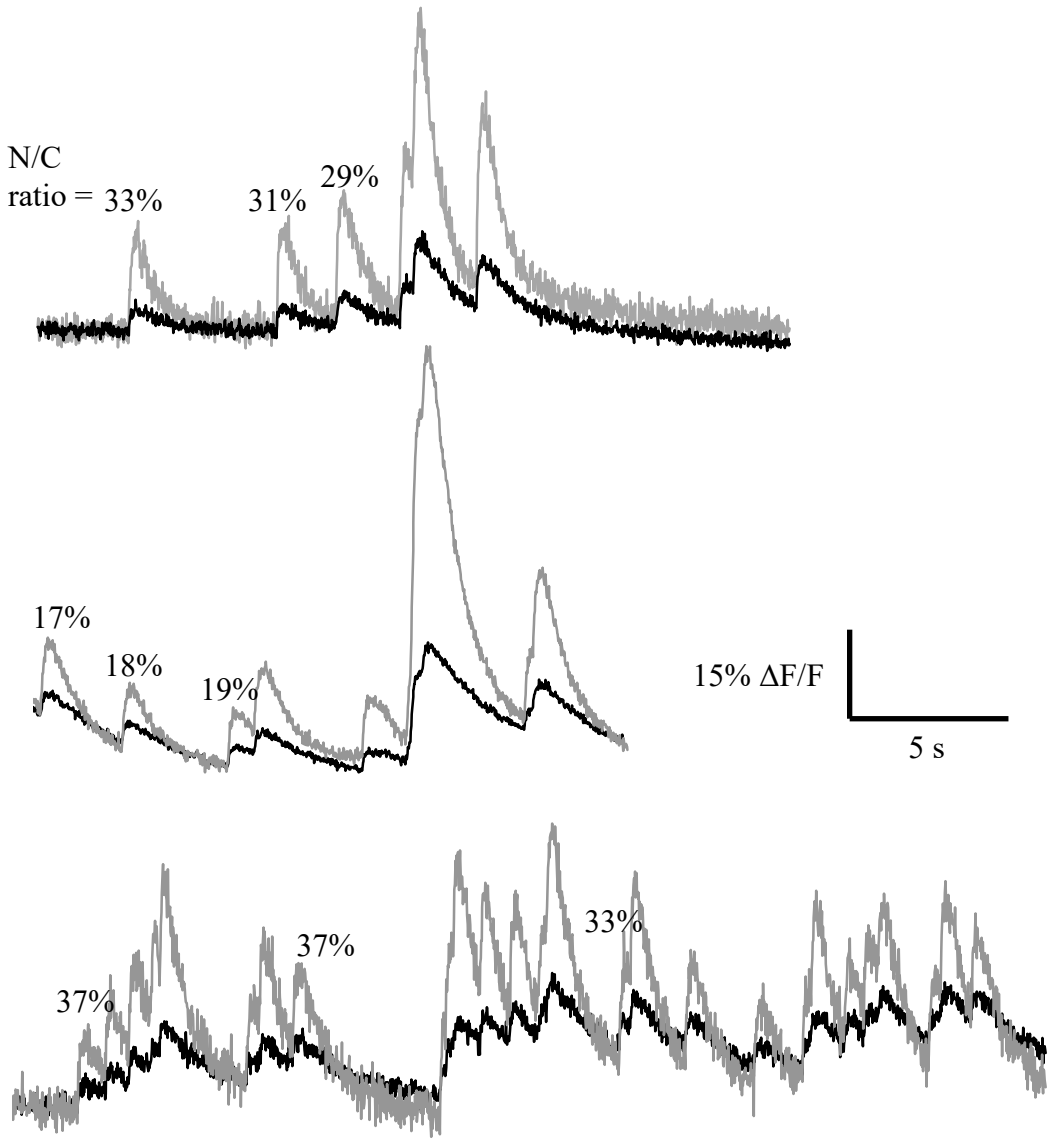

Figure 3.7. *The nuclear/cytosolic relationship associated with single spikes was consistent for the duration of imaging in any one cell*. The nuclear fractional change expressed as percentage of cytosolic fractional change represents the relationship between nuclear and cytosolic Ca^{2+} elevation. This value, indicated above 3 spikes in each trace, remained relatively stable for any one cell for the duration of imaging.

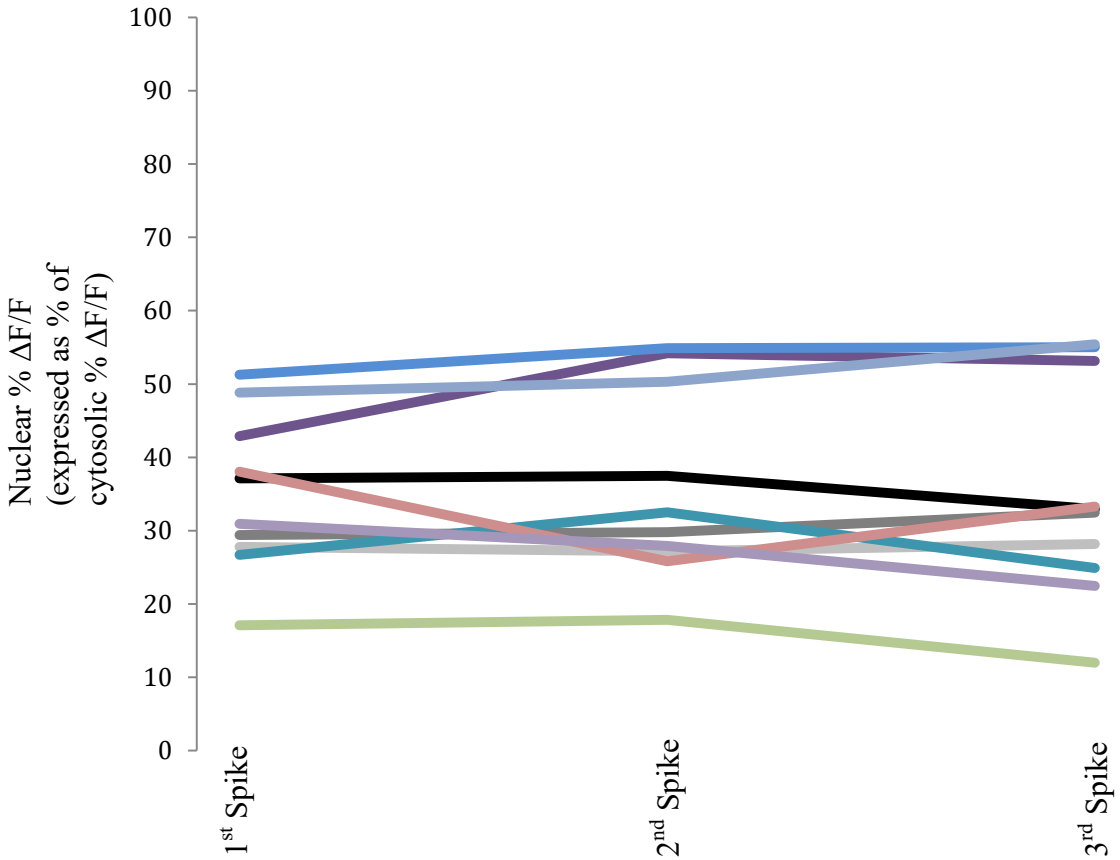

Figure 3.8. *Summary data showing the stability of the nuclear/cytosolic relationship for the duration of imaging in any one cell*. Three spikes picked at random from the traces obtained after imaging each cell showed that the nuclear fractional change expressed as percentage of cytosolic fractional change was relatively robust for each cell (n=10).

3.2.3 Rapid trains of calcium spikes lead to a shift in the nuclear/cytosolic relationship

We consistently found that the nuclear fractional change (expressed as percent of cytosolic fractional change) during trains of spikes was significantly higher (89.40 ± 1.77%) than during single spikes (42.05 ± 7.46%) for each cell ($n=10$; $p<0.05$). Figure 3.9 shows traces demonstrating that the nuclear fractional change (expressed as percent of cytosolic fractional change) pre- to post-build-up is larger than the fractional change at the level of a single spike.

For example, the first spike in trace 1 shows a fractional change in the nucleus that is 43% of the fractional change in the cytosol. Measuring the total change between the starting baseline and the peak of the final transient, however, the nuclear fractional change is 91% of the cytosolic change. These values are labeled in all traces, and are summarized graphically in Figure 3.10.

It is important to point out that representing changes in Ca^{2+} levels in the nucleus as a percentage of change in the cytosol is simply a way to conceptualize the relationship between these two compartments. In reality, the important physiological underpinning is not the change in the ratio *per se*, but that there are key differences in the ability of the cytosol and nucleus to undergo build-up. This is particularly of interest in the context of transcription-dependent changes in neuronal activity, in that certain plasticity-related genes have been shown to require increased and prolonged elevations in nuclear Ca^{2+} (Bading, 2013), a topic that is elaborated upon in Section 4.

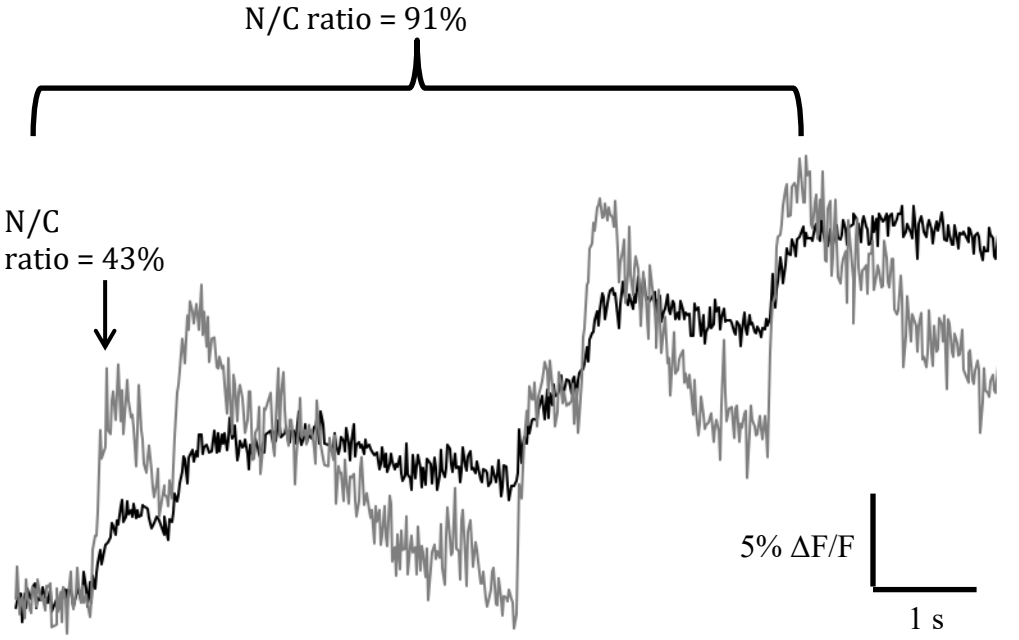
N/C ratio = 91%
N/C
ratio = 43%
5% ΔF/F
1 s

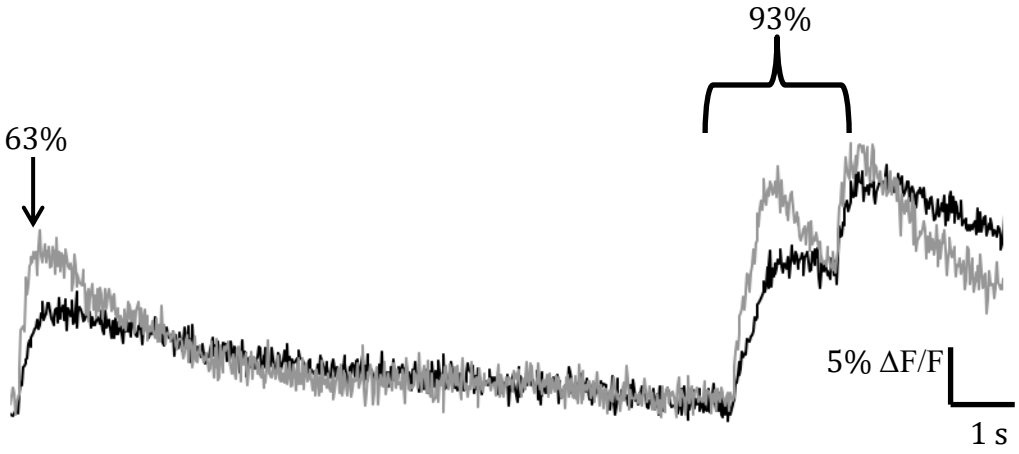
93%
63%
5% ΔF/F
1 s

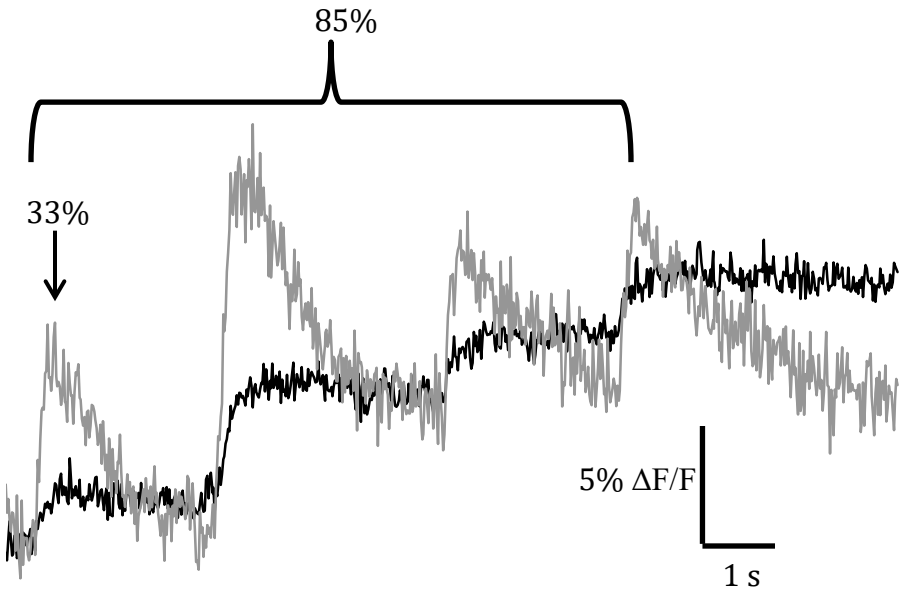
85%
33%
5% ΔF/F
1 s

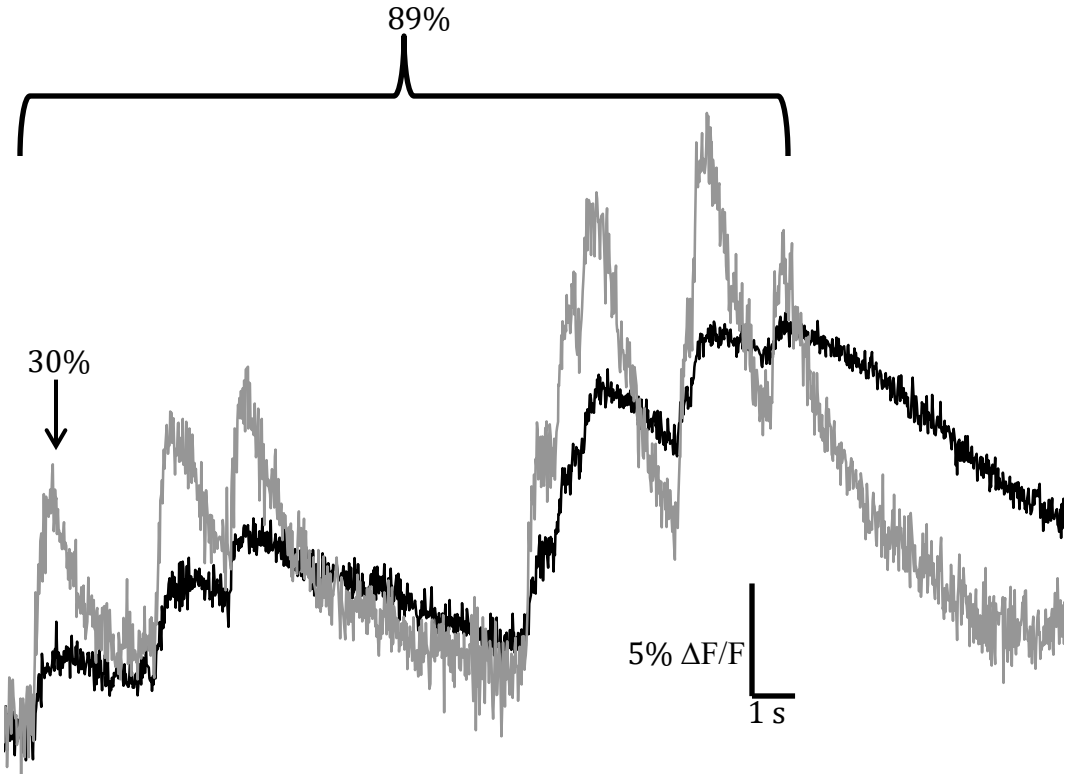
89%
30%
5% ΔF/F
1 s

Figure 3.9. *Representative traces showing the shift in the nuclear/cytosolic relationship when measured for a single spike vs. a train of spikes*. In each trace, the nuclear fractional change expressed as percentage of cytosolic fractional change is substantially larger when calculated for a train of spikes relative to a single spike, indicating that nuclear Ca^{2+} builds up more readily than cytosolic Ca^{2+} under these circumstances.

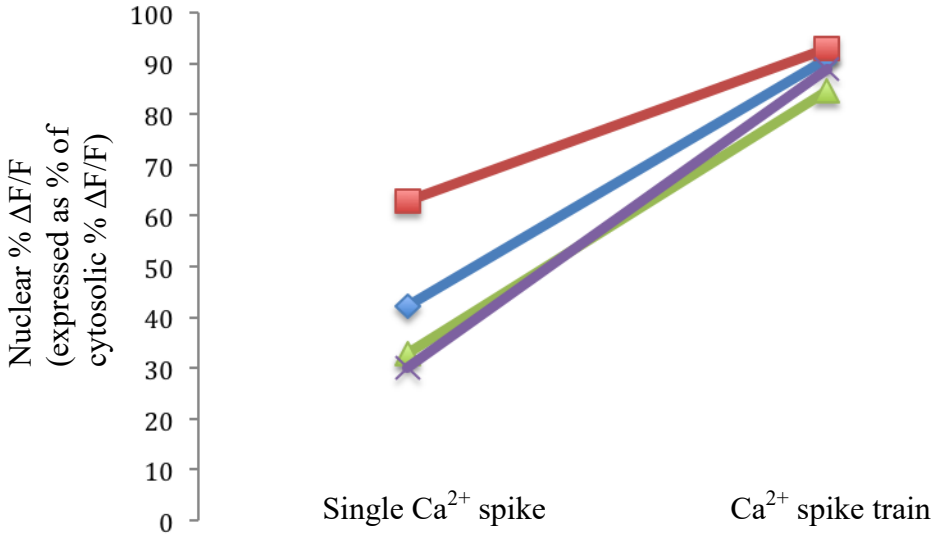

Figure 3.10. *Summary data for the comparison of nuclear/cytosolic relationships for single Ca^{2+} spikes vs. spike trains*. In all 4 cells represented in Figure 3.9, the nuclear fractional change expressed as percent of cytosolic fractional change for a single spike (data points at left; 42.05 ± 7.46%) was significantly smaller than when measured for the fractional change associated with the total rise from baseline to the peak of a train of spikes (data points at right; 89.40 ± 1.77%).

3.3: Pharmacological manipulation of intracellular calcium store uptake and release mechanisms

3.3.1 Inactivation of SERCA pumps and depletion of calcium stores

Given that the relatively stable nuclear/cytosolic relationship we measured for single spikes (Section 3.2.2) could be the result of passive diffusion of Ca^{2+} through nuclear pores or a combination of diffusion and direct release from the NE, we asked whether bath application of CPA, which inactivates SERCA pumps and depletes stores (Soler et al., 1998), could alter this relationship. Our reasoning was that if NE-mediated release was in fact at play, depleting the NE would lead to the subtraction of this component from nuclear Ca^{2+} elevations, leading to a change in the nuclear/cytosolic relationship.

For each cell, we measured the nuclear fractional change (expressed as percent of cytosolic fractional change), incubated the cell in 30 μM CPA for 20 minutes, and measured the post-drug nuclear fractional change (expressed as percent of cytosolic fractional change). Figure 3.11 shows that relative to control, the pre- to post-CPA change in nuclear fractional change was not significantly different from control (n=5; $p>0.05$).

To confirm that our protocol did in fact lead to store depletion, we made use of caffeine, which normally leads to robust RyR-mediated Ca^{2+} release from internal stores (Shmigol et al., 1994). Figure 3.12 shows traces demonstrating the typical response to bath application of 5 mM caffeine in comparison to caffeine application after incubation with CPA, in which the response was completely abolished (n=5).

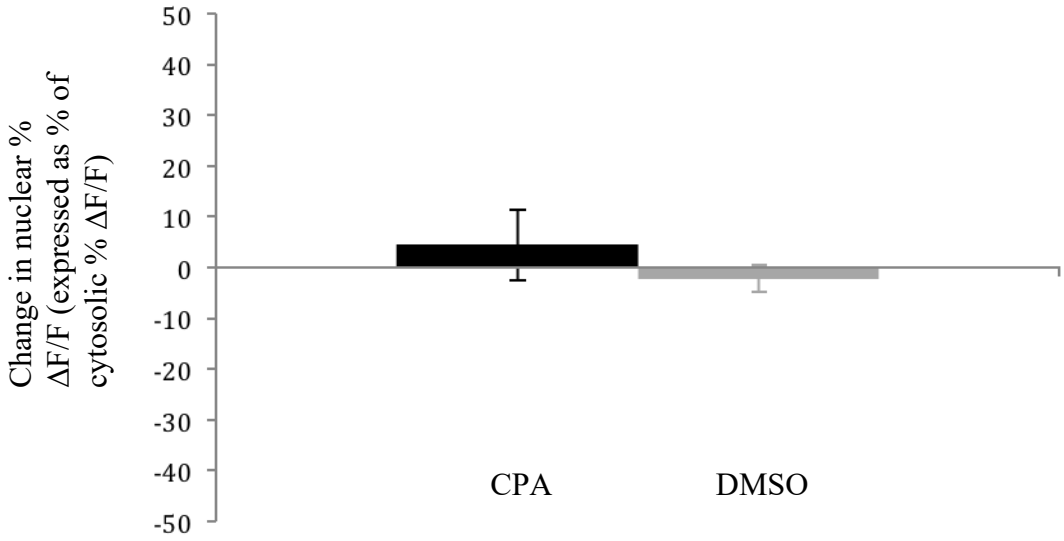

Figure 3.11. *Inactivation of SERCA pumps and store depletion has no effect on the nuclear/cytosolic relationship*. Incubation with CPA did not lead to a significant change (n=5; $p>0.05$) in nuclear Ca^{2+} fractional change (expressed as percentage of cytosolic change) compared to control (DMSO).

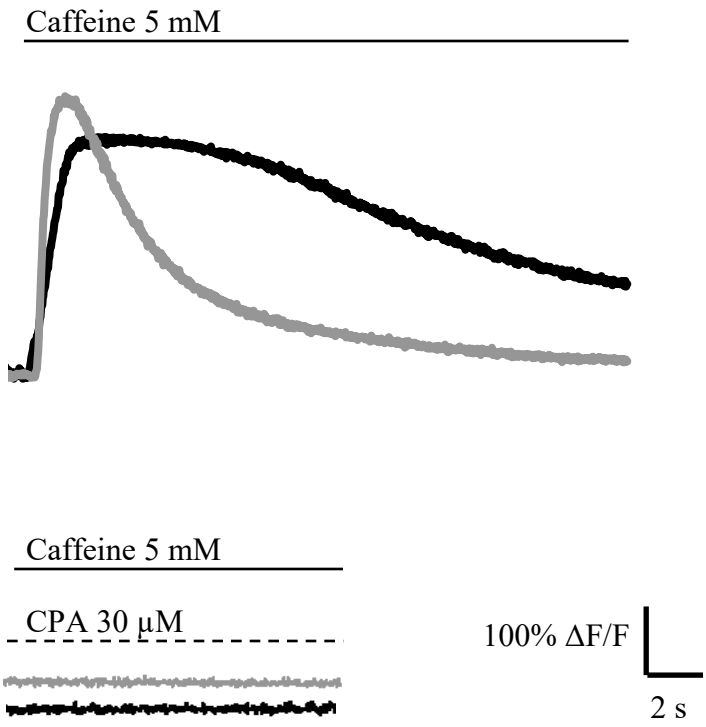

Figure 3.12. *Incubation with CPA depletes stores and abolishes the response to caffeine.* Bath application of 5 mM caffeine typically induces a robust response (top) in both the cytosol (grey) and nucleus (black). Caffeine application after 20 min incubation with 30 µM CPA produced no response (bottom).

In interpreting the lack of an effect by CPA, it is important to note that a major mechanism of Ca^{2+} clearance from the nucleoplasm is diffusion back out of the nuclear pore complexes, driven by rapid uptake by SERCA pumps on the extranuclear ER (Brini et al., 2013). It is therefore plausible that application of CPA has opposing effects on nuclear Ca^{2+}. Specifically, it could be that by inactivating SERCA pumps and inhibiting their clearance capability, we induced a slight augmenting effect on nuclear Ca^{2+}, and simultaneously, we reduced nuclear Ca^{2+} signals by depleting the NE store. The aggregate effect of this could, in theory, be the negative result we obtained.

To address this possibility, we next looked to specifically manipulate store release mechanisms and determine whether this had an effect on the nuclear/cytosolic relationship.

3.3.2 Inactivation of RyRs

In light of the scarce experimental evidence regarding the presence of RyRs on the NE, we sought to determine whether inactivation of RyRs could alter the observed nuclear/cytosolic Ca^{2+} dynamics.

In this case, we measured the nuclear fractional change for a single spike (expressed as percent of cytosolic fractional change), incubated each cell for 20 minutes with 25-30 μM ryanodine, and measured the post-drug nuclear fractional change (expressed as percent of cytosolic fractional change). At this dose, ryanodine is known to prevent RyR activation (McPherson et al., 1991).

Again, to confirm the efficacy of our pharmacological technique, we bath applied 5 mM caffeine after ryanodine incubation and found that the typical Ca^{2+} response was abolished by the drug (n=5; Figure 3.13).

Figure 3.14 shows that inactivation of RyRs did not result in a significant change in the nuclear fractional change (percent of cytosolic fractional change) compared to control (n=7; $p>0.05$).

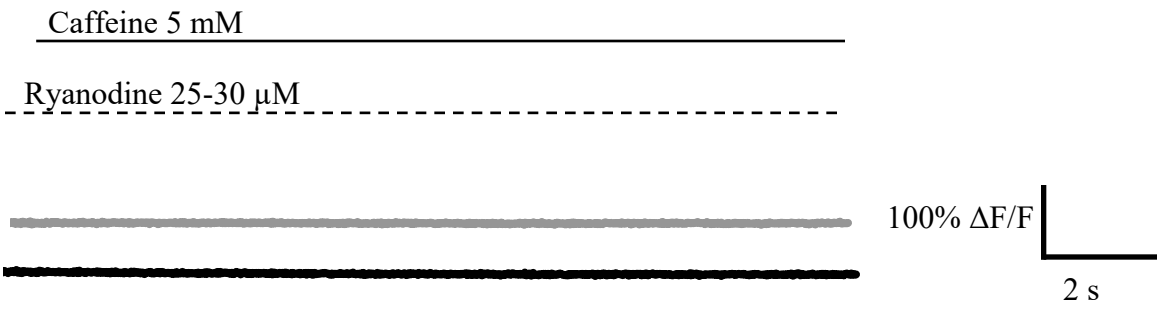

Figure 3.13. *Incubation with ryanodine prevents the response to bath application of caffeine.* 20 min incubation with 25-30 µM ryanodine abolished the Ca^{2+} wave normally induced by bath application of 5 mM caffeine in both the cytosol (grey) and nucleus (black).

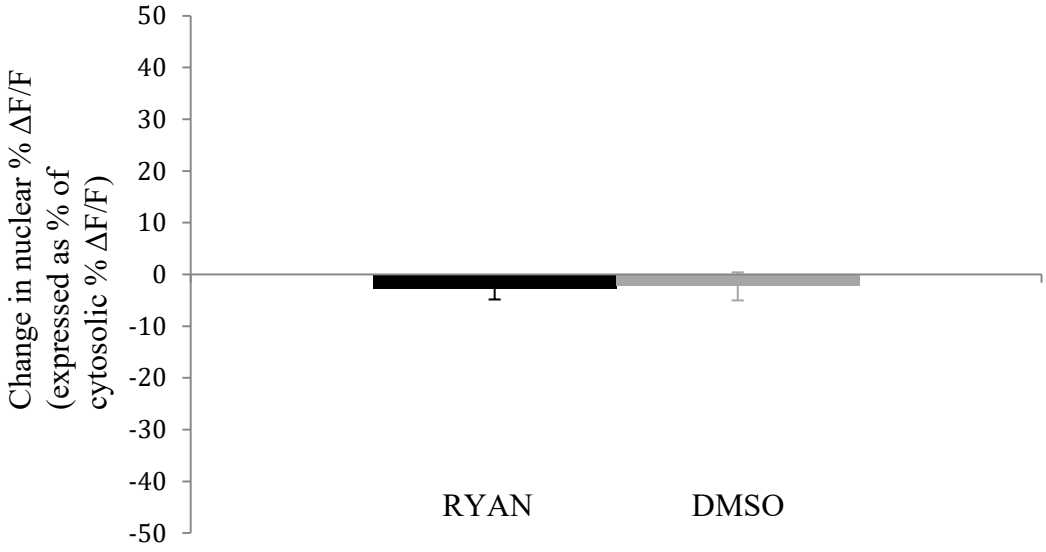

Figure 3.14. *Inactivation of RyRs does not lead to a change in the nuclear/cytosolic calcium relationship.* 20 min incubation with 25-30 μM ryanodine did not significantly alter the nuclear fractional change (expressed as percent of cytosolic fractional change) compared to control (n=7; $p>0.05$).

As previously mentioned, there is evidence to suggest that IP_3Rs may be localized on the inner leaflet of the NE, where they could contribute directly to nuclear Ca^{2+} transients (Bading, 2013). Because of this, we looked to test the possibility of a role for IP_3Rs in the nuclear calcium signals we observed.

3.3.3 Inactivation of IP_3 Receptors

Xestospongin C (XeC), originally isolated from Pacific basin sponges, is known to inhibit IP_3-mediated Ca^{2+} release at the receptor level (Miyamoto et al., 2000). We thus looked to determine whether 10-minute incubation with 5 μM XeC would lead to a change in the nuclear fractional change (expressed as percent of cytosolic fractional change). In this case, we were not able to perform a test for drug efficacy. One possible method of confirming that XeC was effective would have been via comparisons of control vs. post-XeC carbachol application, since bath application of carbachol can activate mAChRs and induce IP_3-dependent Ca^{2+} waves (Power and Sah, 2002). However, we found that, in line with previous studies (Watanabe et al., 2006), carbachol produced inconsistent results, and that inducing global waves was rather difficult. Given that such waves require a coincidence of IP_3 build-up and Ca^{2+} elevation (Watanabe et al., 2006), it may have been that in our dissociated hippocampal cultures, cells typically did not have sufficient IP_3 tone to allow for a reliable effect of carbachol. Nevertheless, we used a XeC protocol that has been shown to cause IP_3R inactivation. Figure 3.15 shows that incubation with XeC did not have a significant effect on nuclear fractional change (expressed as percent of cytosolic fractional change) relative to control ($n=3$; $p>0.05$).

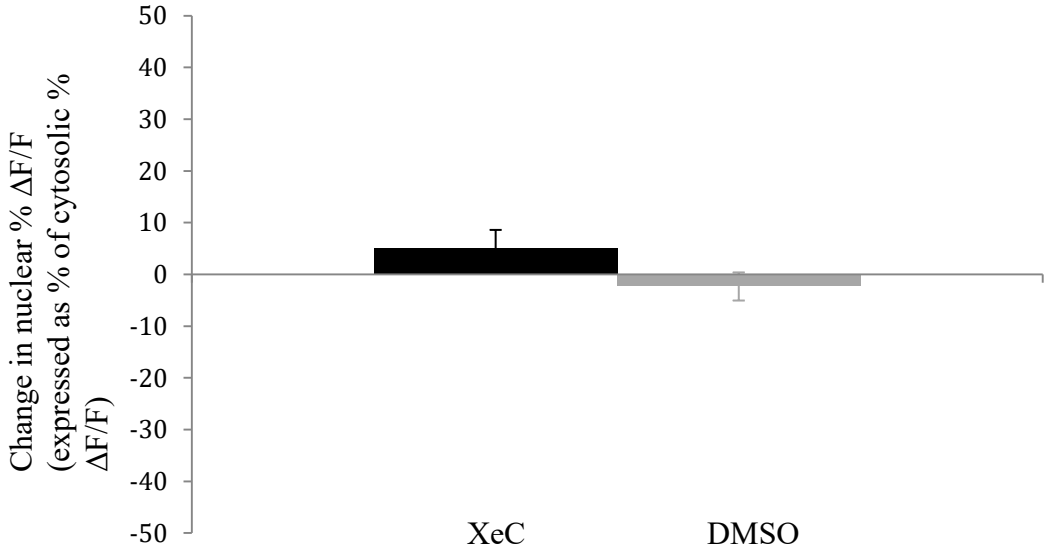

Figure 3.15. *Application of XeC does not lead to a change in nuclear/cytosolic calcium dynamics.* 10 min incubation with 5 μM XeC did not cause a significant change in the nuclear fractional change (expressed as percent of cytosolic fractional change) compared to control (n=3; $p>0.05$).

Taken together, in testing for the possible role of store release in the nuclear Ca^{2+} dynamics we measured, our manipulations of intracellular stores provided compelling evidence that release of Ca^{2+} from the NE's perinuclear space is not an important mechanism for generating the observed nuclear Ca^{2+} signals.

The above experiments addressed the relationship between nuclear and cytosolic Ca^{2+} *spikes*. As previously described, Ca^{2+} spikes differ considerably from waves with respect to both mechanism and function. As such, in a final set of experiments, we turned our attention to cytosolic and nuclear Ca^{2+} dynamics during wave activity.

3.4: Nuclear and cytosolic dynamics during caffeine-induced calcium waves

As previously mentioned, bath application of caffeine induces a global Ca^{2+} wave (via CICR) that is dependent on RyRs (Shmigol et al., 1994). RyR-mediated CICR has been studied extensively, and continues to draw attention in the context of amplification of Ca^{2+} signals that may be implicated in plasticity mechanisms.

What remains unclear, however, is whether Ca^{2+} release from RyRs *alone*, with no contribution from IP_3Rs, is sufficient to generate and propagate these global waves. As an analogy, IP_3R-dependent Ca^{2+} waves have been shown to be unchanged in the presence of a concentration of ryanodine sufficient to inactivate RyRs (Raymond and Redman, 2006). Given the overlapping expression patterns of these two receptor types, it is important to address their independence from or cooperation with one another to clarify their mechanistic details.

We therefore looked to determine whether RyR-dependent waves induced by caffeine are affected by inactivation of IP_3Rs with XeC.

First, we showed that bath application of 5 mM caffeine alone resulted in a Ca^{2+} wave that propagated through the soma and invaded the nucleus (Figures 3.16 and 3.17). The average fractional change measured in the cytosol was 424.8 ± 92.1 %, while the response in the nucleus was 123 ± 25.5 % (Figure 3.18, left, n=5 for both). The invasion of the nucleus was associated with a kinetic delay: the average rise time was 1.04 ± 0.09 s in the cytosol and 2.9 ± 0.60 s in the nucleus (Figure 3.19, left; n=5 for both).

To test whether this dynamic was changed by the inactivation of IP_3Rs, we repeated this experiment after 10 min incubation with 5μM XeC. Post-XeC caffeine-induced waves were not significantly different from control caffeine waves. Figure 3.18 shows that there was no effect with respect to Ca^{2+} wave amplitude. The average cytosolic and nuclear wave amplitudes were 323.3 ± 25.4 % and 157.8 ± 11.6 %, respectively (n=3 for both), which were not significantly different from amplitudes measured for control caffeine-induced waves ($p>0.05$). The rise times associated with these waves, shown in Figure 3.19, were 0.903 ± 0.093 s in the cytosol and 3.4 ± 0.300 s in the nucleus (n=4 for both), and were again not significantly different from rise times of control caffeine-induced waves ($p>0.05$).

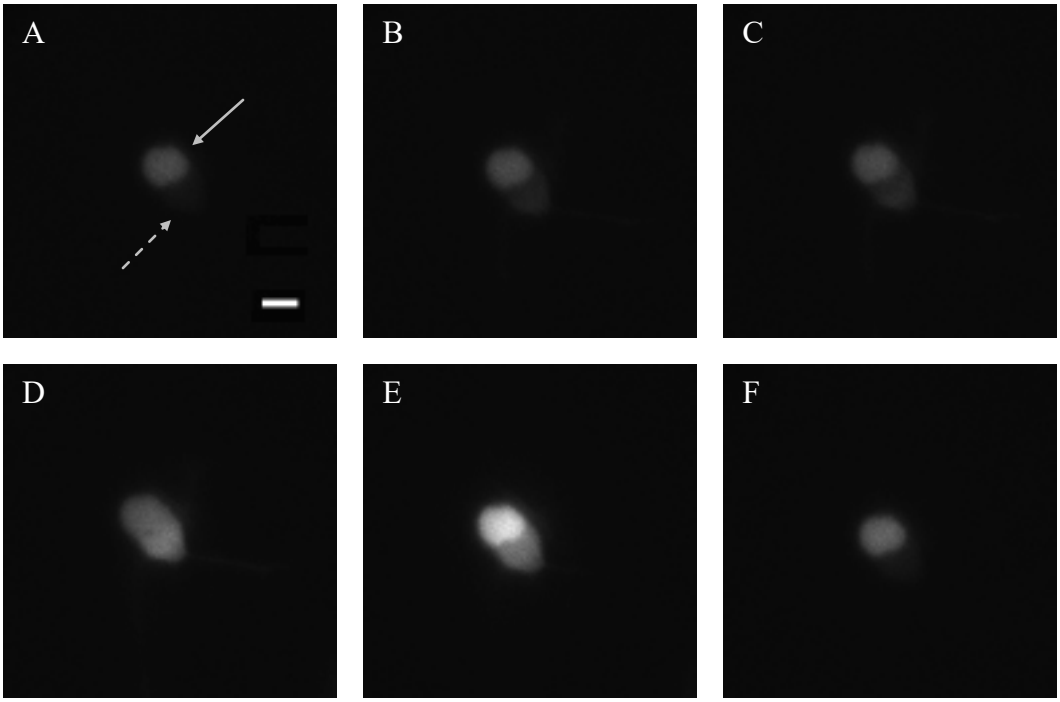

Figure 3.16. *Propagation of a global caffeine-induced wave from the cytosol to the nucleus.* Bath application of 5 mM caffeine to a cell initially at rest (A; dashed arrow indicates extranuclear soma and solid arrow indicates nucleus) triggered a Ca^{2+} wave (B) that propagated through the soma (C and D) and invaded the nucleus (E), after which both nuclear and cytosolic fluorescence signals began to return to baseline (F). Scale bar = 10 μm.

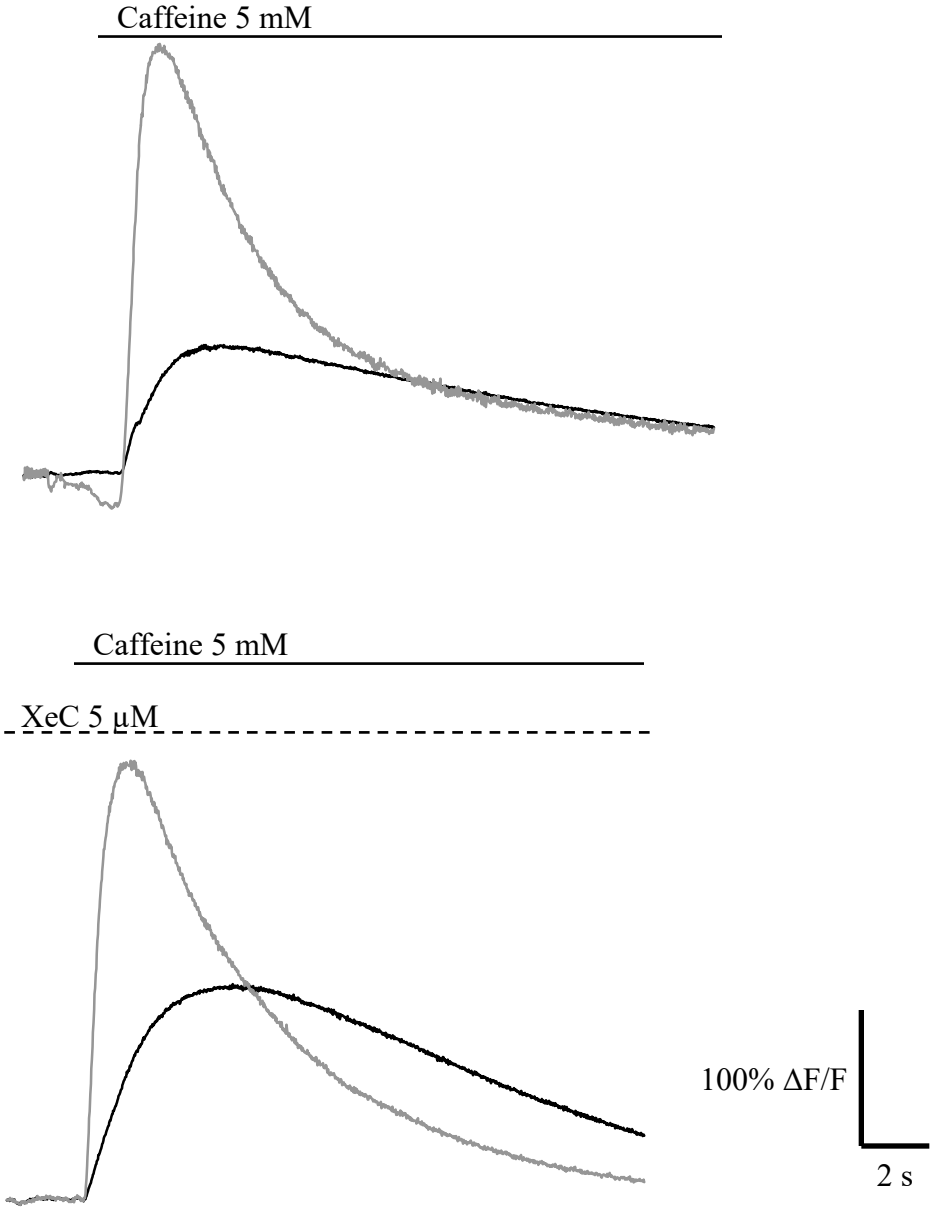

Figure 3.17. *Inactivation of IP_3Rs with XeC does not affect the cytosolic or nuclear response to caffeine-induced waves.* Representative traces of a control response to caffeine (top) and a caffeine-induced wave after 10 min incubation with 5 µM XeC (bottom). Application of XeC did not inhibit the nuclear (black) or cytosolic (grey) response to caffeine.

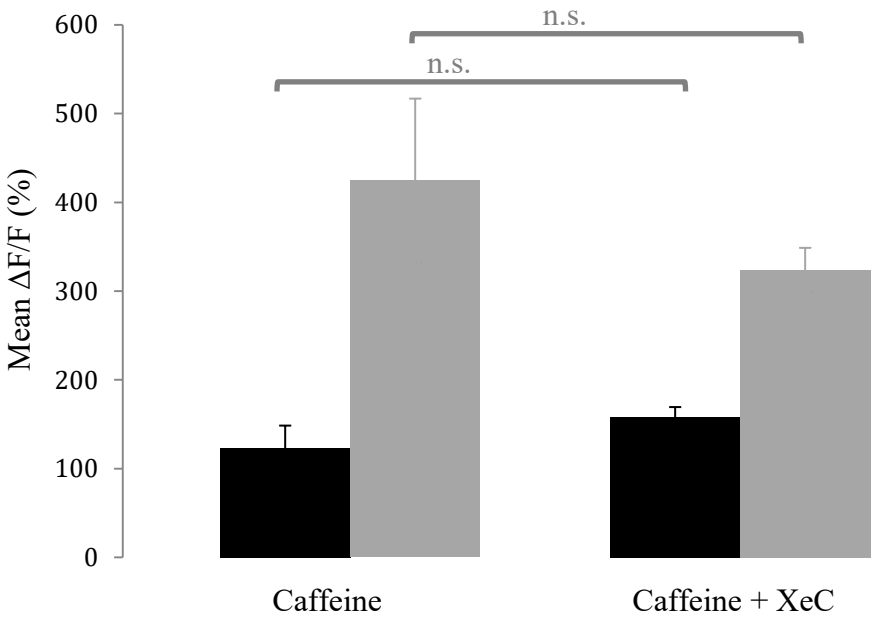

Figure 3.18. *Nuclear and cytosolic caffeine-induced wave amplitudes are unchanged by inactivation of IP_3Rs.* Average fractional change in nucleus (black) and cytosol (grey) under control conditions (left) are not significantly different ($p>0.05$) from those induced by caffeine after incubation with XeC (right).

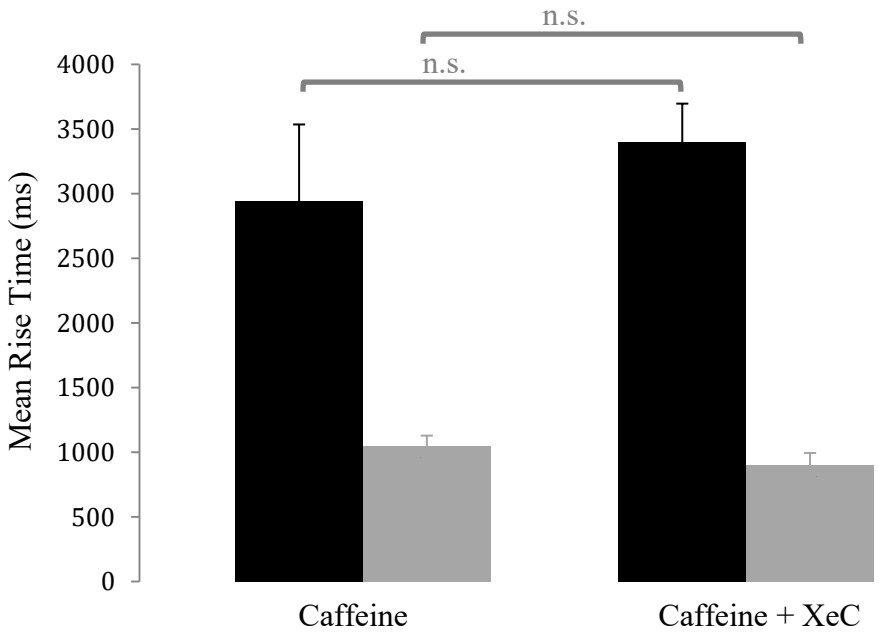

Figure 3.19. *Rise time of caffeine-induced waves is unchanged by inactivation of IP_3Rs.* Average rise times in the nucleus (black) and cytosol (grey) under control conditions (left) are not significantly different ($p>0.05$) from those induced by caffeine after incubation with XeC (right).

CHAPTER 4

Discussion

4.1 Overview of Main Findings

By visualizing cytosolic and nuclear Ca^{2+} spikes simultaneously during spontaneous activity in dissociated hippocampal neurons, we were able to report on the differences between these two compartments with regards to the amplitude and kinetics of Ca^{2+} elevations. Consistent with prior experiments (Power and Sah, 2002), we found that nuclear transients were smaller in amplitude and displayed slower kinetics compared to cytosolic transients. To establish a measure of the nuclear/cytosolic relationship, we expressed the fractional change in the nucleus as a percentage of the fractional change in the cytosol during Ca^{2+} spikes. We found that this measure stayed relatively stable across individual spikes for any one cell. In the case of rapid build-up of multiple spikes however, the total fractional change from baseline to the peak of the build-up was associated with significantly different nuclear/cytosolic relationships: the fractional change in the nucleus grew much closer to the fractional change in the cytosol.

Given that this nuclear/cytosolic relationship could be purely a result of Ca^{2+} diffusion from the cytosol through the nuclear pores, or in part amplified by direct Ca^{2+} release from the perinuclear NE, we next inactivated SERCA pumps and depleted stores and found that this did not affect the nuclear/cytosolic relationship significantly. Similarly, inactivation of RyRs, and in separate experiments, inactivation of IP_3Rs, did not lead to significant fluctuations in this dynamic. Together, these experiments provided evidence

that the nuclear/cytosolic relationship we observed was predominantly a result of diffusion of Ca^{2+} from the cytosol.

Finally, we turned our focus to Ca^{2+} waves known to be dependent on cytosolic RyRs. We demonstrated that inactivation of IP_3Rs does not impact the amplitude or kinetics of RyR-mediated Ca^{2+} elevation in the soma or nucleus, indicating that this mechanism is capable of independently generating and carrying Ca^{2+} waves to the nucleoplasm.

4.2 Experimental Paradigm

4.2.1 Use of cytosolic- and nuclear-targeted GECIs

Making use of GCaMPs allowed us to restrict the Ca^{2+} response of each sensor specifically to the cytosol (mCherry-GCaMP6f) and nucleus (GCaMP7-NLS). In contrast, studies using fluorescent dyes often use the differential accumulation of dye in the two compartments to distinguish between these signals, which can lead to ambiguity with respect to the source of observed signals in certain cases. Further, we used two of the fastest and most sensitive GCaMPs currently available, which helped resolve modest Ca^{2+} signals.

However, the use of GCaMPs did present inherent drawbacks. First, one of the fundamental limitations of these GECIs in comparison to dyes is that they cannot be easily calibrated in a reliable way (Bootman et al., 2009). We therefore did not report absolute Ca^{2+} concentrations, and focused instead on the *relative* relationship between nuclear and cytosolic Ca^{2+} signals.

Further, the use of GECIs leaves open the possibility of different levels of expression of the sensors between cells. In our case, it is possible that either one or both sensors were expressed at slightly different levels between cells. One possible ramification of this would have been high variability in when making comparisons of single spikes between cells, for instance. However, in measuring average nuclear and cytosolic fractional changes associated with individual spikes from different cells, we found relatively low variability and relatively consistent results for each compartment (11.1-13.5% in the cytosol and 3.75-4.67%% in the nucleus), suggesting that any expression differences did not significantly jeopardize our ability to make these measurements. This applies to our data corresponding to amplitudes associated with caffeine-induced waves as well. In the case of analyzing fractional changes for single spikes vs. build-ups, or measuring the effects of store manipulations, all comparisons were made within each cell, and so expression issues were not a concern.

It is also important to note the possible issues associated with the use of different sensors in the cytosol and nucleus. For example, GCaMP7 produces brighter signals relative to GCaMP6f (Podor et al., 2015). Considering that our data showed smaller fractional changes in the nucleus than in the cytosol, however, we conclude that this inherent difference in the sensors did not prevent us from detecting the physiological nuclear/cytosolic relationship. Additionally, it is known that GCaMP6f has faster kinetics than GCaMP7 (Podor et al., 2015). Comparisons of the two sensors in hippocampal neuron dendrites showed that GCaMP6f has a time constant (τ_{on}) that is on average 5 ms faster than that of GCaMP7. This difference, however, is relatively small, and given that

we reported substantially larger differences between cytosolic and nuclear Ca^{2+} signal rise times, we are confident that our measurements were primarily of the underlying physiology as opposed to sensor differences.

4.2.2 Lack of electrical recording

A limitation in our study was the lack of simultaneous recording of electrical activity. Because of this, we were unable to address directly the exact nature of the electrical activity associated with our observed Ca^{2+} spikes. However, given that the single spikes we measured were associated with a consistently modest fractional change and relatively fast rise time, we hypothesize that we were observing Ca^{2+} spikes induced by one or a few action potentials based on previous reports (Bengtson et al., 2010).

Because of this uncertainty, and because we typically observed different types of Ca^{2+} elevations during any one experiment (e.g. single spikes and large elevations made of many spikes built up on one another), we had to devise a way of measuring nuclear and cytosolic Ca^{2+} spikes that would allow for valid comparisons before and after store manipulations. We chose to measure the smallest spike observed in each trace. This allowed us to remain consistent for the reasons outlined in Section 3.2: the smallest spike was a relatively stable phenomenon across experiments with respect to amplitude and kinetics (demonstrated by the relatively low variability in our measures of the average amplitude and kinetics of single spikes measured in different cells).

4.3 The nuclear/cytosolic relationship is different at the level of single calcium spikes and spike build-ups

As a method of quantifying the *relative* degree of Ca^{2+} elevation in the nucleus vs. the cytosol, we reported the fractional change ($\Delta F/F$) in the nucleus as a percentage of $\Delta F/F$ in the cytosol. Tracking this measure for single spikes throughout the duration of imaging in any one cell, we found that it remained relatively stable. This had two important implications. First, it generated the question of whether or not the underlying mechanism was in part dependent on some form of constitutive NE store release, which led to the experiments covered in Section 3.3 and discussed in the following section. Second, it showed a striking difference when compared to the nuclear/cytosolic relationship at the level of Ca^{2+} elevations induced by trains of spikes.

The fractional change in the nucleus when expressed as a percentage of cytosolic fractional change was significantly larger in response to a build-up of Ca^{2+} spikes compared to a single spike. The representative traces in Section 3.2.3 show that this was a result of the slower decay rate in the nucleus, such that when spikes occurred with relatively high frequency, the nucleus accumulated Ca^{2+} more readily than the cytosol. This is especially of interest in the context of transcription-dependent forms of LTP. Many lines of evidence have pointed to the necessity of nuclear Ca^{2+} elevation for L-LTP (Bading, 2013). Prolonged periods of Ca^{2+} elevation in the nucleus have been shown to be required to activate the signalling cascades that involve upregulation of CaM kinases (CaMKs), which are known to be important for L-LTP (Adams and Dudek, 2005). Given that a typical stimulation protocol for inducing L-LTP involves multiple 100 Hz tetani,

the unique ability of the nucleus to undergo frequency-dependent build-up of Ca^{2+} may be at play in the conversion of these electrical inputs to the nuclear Ca^{2+}-dependent transcriptional cascades necessary for L-LTP.

Apart from the observed kinetic differences between the cytosol and nucleus, an important question relating to our observations had to do with the presence or absence of perinuclear Ca^{2+} contribution, and led to our manipulations of store release and uptake mechanisms.

4.4 Lack of evidence for direct contribution from the perinuclear space to nuclear calcium spikes

Evidence for and against a role for release from the NE in the generation of nuclear Ca^{2+} transients in neurons has been mixed. Moreover, in certain experiments that have shown nuclear signals to decrease upon depletion of intracellular stores (Hardingham et al., 2001), a simultaneous measure of cytosolic Ca^{2+} was missing, and thus it cannot be determined whether the observed effect was due to disruption of an NE-mediated mechanism or simply a spillover effect of reduced cytosolic transient amplitudes. Our imaging paradigm provided the advantage of tracking Ca^{2+} activity in both compartments, and we were thus better able to address the cytosolic/nuclear interface more directly.

By using CPA to deplete intracellular stores, and by targeted inactivation of RyRs and IP_3Rs, we showed that Ca^{2+} from stores was not an important aspect of the dynamics we

observed. Specifically, because the nuclear fractional change (expressed as percent of cytosolic fractional change) did not differ significantly pre- and post-drug, our findings show evidence against a role for direct NE-mediated release in the observed nuclear Ca^{2+} elevations.

Our results are in line with prior reports of store-independent Ca^{2+} spikes in hippocampal neurons. Bengtson et al. (2010) showed that in response to high frequency stimulation (HFS), nuclear Ca^{2+} signals were unaffected by the depletion of stores using CPA. Moreover, combining the results from our store-related experiments and observations of Ca^{2+} spike frequency-dependent build-up in the nucleus leads to potentially interesting implications related to L-LTP. There is evidence to suggest that unlike E-LTP, which is associated with store-related Ca^{2+} dynamics in dendritic spines (Emptage et al., 1999), L-LTP is heavily dependent on VGCC-mediated Ca^{2+} influx and seemingly independent of store release (Raymond and Redman, 2006). Considering that L-LTP is known to require nuclear Ca^{2+}-dependent transcription, it may be that our observation of build-up in the nucleus, and lack of store-dependence in our Ca^{2+} dynamics, is representative of one method by which L-LTP can be induced by high frequency somatic Ca^{2+} spikes (and not regenerative release from stores).

Nevertheless, as already pointed out there have been studies that demonstrate a role for store release in generating nuclear Ca^{2+} transients. For example, nuclear Ca^{2+} spikes induced by bicuculline and linked to CREB phosphorylation have been shown to arise when backpropagating action potentials trigger regenerative, store-dependent waves that

begin in the dendrite and propagate to the nucleus (Hardingham et al., 2001). These signals were observed to decrease after incubation with CPA. Again, however, without simultaneous visualization of cytosolic Ca^{2+}, this study did not address the idea of direct release from the NE to the nucleoplasm.

Several possible reasons may underlie the discrepancy between studies showing a role for store release and those (including ours) that suggest store-independent nuclear Ca^{2+} elevations. First, intracellular stores may be primed to different degrees by experimental conditions such as cell types and stimulation protocols. For example, the bicuculline-induced nuclear signals reported by Hardingham et al. (2001) were associated with a longer timescale relative to the HFS-evoked transients observed by Bengtson et al. (2010), and thus may represent larger elevations that are sufficient to recruit stores. Relatedly, the spontaneous spikes we have reported may be too small to evoke store release. Specifically, given that IP_3R activation requires sufficient store Ca^{2+} levels, build-up of cytosolic IP_3 and elevated cytosolic Ca^{2+} (Barbara, 2002), our paradigm may have been insufficient to trigger IP_3R activity. Ryanodine receptors are also dependent on interactions with cytosolic modulators as well as store and cytosolic Ca^{2+} levels, but are typically known to be activated more readily than IP_3Rs (Zalk et al., 2007). In this case, our experiments may have again involved activity that was insufficient to trigger RyR-mediated release. Alternatively, it may be that while store release was involved, its contribution to the observed transients was so minor relative to influx through VGCCs that it was undetectable in our analyses.

Broadly speaking, the emerging view is that the contribution of stores to nuclear Ca^{2+} signals may be state-dependent, playing a role under certain circumstances and remaining uninvolved (or at least minimally involved) in others. In this respect, our results demonstrate another case in which nuclear signals, even those that are capable of undergoing build-up, can arise without release from stores.

4.5 Sufficiency of RyRs in the generation and propagation of global calcium waves

The function of global RyR-mediated CICR is still largely unclear. Although it has been demonstrated that RyRs can potentiate somatic Ca^{2+} transients induced by action potentials (Sandler and Barbara, 1999), what purpose may be served by Ca^{2+} waves that are triggered and carried by RyRs remains to be revealed. In fact, to our knowledge, there have been no direct tests of the ability of RyRs to propagate waves globally, without IP_3R contribution. This was the driving force behind our final experiments, in which we provided the first account of GECI-based cytosolic and nuclear signals during caffeine-induced Ca^{2+} waves. We showed that after inactivating IP_3Rs, RyR-dependent waves elicited by caffeine were not impeded (in amplitude or kinetics) in propagating to and invading the nucleus.

This may have implications relating to the generation of large nuclear signals, such as those linked to activity-dependent transcription cascades. Given what is already known about RyR-mediated potentiation of action potential-induced Ca^{2+} spikes (Sandler and Barbara, 1999), our findings provide evidence that at least from the standpoint of release capability – i.e. their ability to act as functional store release sites in the soma and around

the nucleus without involvement of IP_3Rs - RyRs may under certain conditions be responsible for an augmenting mechanism that involves the nucleus as well.

4.6 Conclusions and Future Directions

Taken together, our findings highlight the relationship between cytosolic and nuclear Ca^{2+} dynamics. Most importantly with respect to the generation of nuclear Ca^{2+} signals, they provide an example of spike activity that is not dependent on perinuclear Ca^{2+} as well as wave activity that is driven only by RyRs without IP_3R involvement.

A natural continuation of this work is to employ the concept of simultaneous cytosolic and nuclear Ca^{2+} imaging to search for conditions in which perinuclear Ca^{2+} may be of significance. Just as store release from the ER has been shown to play an important role in augmenting Ca^{2+} and thus triggering distinct signalling cascades in the cytosol, it needs to be determined whether release from the NE to the nucleoplasm serves as a distinguishing factor, perhaps in the context of persistent forms of LTP.

Imaging cytosolic and nuclear Ca^{2+} signals in response to Ca^{2+} spikes, RyR- and IP_3R-mediated waves and during pharmacological manipulation of intracellular stores is an effective starting point for studying the different mechanisms of Ca^{2+} entry into the nucleus. Such paradigms can be made even more revealing by the use of recently developed ER Ca^{2+} sensors such as GCaMPer (Henderson et al., 2015), which could visualize decreases in perinuclear Ca^{2+} associated with release from the NE to the nucleus. Combining this with gene readouts will more specifically address transcription-

dependent forms of LTP. It has already been established that nuclear Ca^{2+} signals are important for LTP-related gene regulation; revealing how they are generated by distinct mechanisms under different conditions may be one of the most critical aspects of studying transcription-dependent plasticity.

REFERENCES

Adams, J. P., & Dudek, S. M. (2005). Opinion: Late-phase long-term potentiation: Getting to the nucleus. *Nature Reviews Neuroscience Nat Rev Neurosci, 6*(9), 737-743.

Ahlijanian, M. K., Westenbroek, R. E., & Catterall, W. A. (1990). Subunit structure and localization of dihydropyridine-sensitive calcium channels in mammalian brain, spinal cord, and retina. *Neuron, 4*(6), 819-832.

Ahrens, M. B., Orger, M. B., Robson, D. N., Li, J. M., & Keller, P. J. (2013). Whole-brain functional imaging at cellular resolution using light- sheet microscopy. *Nature Methods, 10*(5), 413.

Bading, H. (2013). Nuclear calcium signalling in the regulation of brain function. *Nature Reviews Neuroscience Nat Rev Neurosci, 14*(9), 593-608.

Bano, D., Young, K. W., Guerin, C. J., Lefeuvre, R., Rothwell, N. J., Naldini, L., . . . Nicotera, P. (2005). Cleavage of the Plasma Membrane Na /Ca2 Exchanger in Excitotoxicity. *Cell, 120*(2), 275-285.

Barbara, J. (2002). IP3-dependent calcium-induced calcium release mediates bidirectional calcium waves in neurones: Functional implications for synaptic plasticity. *Biochimica Et Biophysica Acta (BBA) - Proteins and Proteomics, 1600*(1-2), 12-18.

Beck, M., Förster, F., Ecke, M., Plitzko, J. M., Melchior, F., Gerisch, G., Baumeister, W., & Medalia, O. (2004). Nuclear pore complex structure and dynamics revealed by cryoelectron tomography. *Science (New York, N.Y.), 306*(5700), 1387.

Bengtson, C. P., & Bading, H. (2012). Nuclear Calcium Signaling. *Synaptic Plasticity Advances in Experimental Medicine and Biology,* 377-405.

Bengtson, C. P., Freitag, H. E., Weislogel, J., & Bading, H. (2010). Nuclear Calcium Sensors Reveal that Repetition of Trains of Synaptic Stimuli Boosts Nuclear Calcium Signaling in CA1 Pyramidal Neurons. *Biophysical Journal, 99*(12), 4066-4077.

Berridge, M. J. (1998). Neuronal Calcium Signaling. *Neuron, 21*(1), 13-26.

Berridge, M. J. (2000). The Versatility and Complexity of Calcium Signalling. *Novartis Foundation Symposia Complexity in Biological Information Processing,* 52-67.

Blaustein, M., & Lederer, W. (1999). Sodium/ calcium exchange: Its physiological implications. *Physiological Reviews, 79*(3), 763-854.

Blaustein, M. P., & Golovina, V. A. (2001). Structural complexity and functional diversity of endoplasmic reticulum Ca2 stores. *Trends in Neurosciences, 24*(10), 602-608.

Bootman, M. D., Fearnley, C., Smyrnias, I., Macdonald, F., & Roderick, H. L. (2009). An update on nuclear calcium signalling. *Journal of Cell Science, 122*(14), 2337-2350.

Bootman, M., Harzheim, D., Smyrnias, I., Conway, S., & Roderick, H. (2007). Temporal changes in atrial EC-coupling during prolonged stimulation with endothelin-1. *Cell Calcium, 42*(4-5), 489-501.

Brini, M., & Carafoli, E. (2010). The Plasma Membrane Ca^{2+} ATPase and the Plasma Membrane Sodium Calcium Exchanger Cooperate in the Regulation of Cell Calcium. *Cold Spring Harbor Perspectives in Biology, 3*(2).

Brini, M., Calì, T., Ottolini, D., & Carafoli, E. (2013). Intracellular Calcium Homeostasis and Signaling. *Metal Ions in Life Sciences Metallomics and the Cell,* 119-168.

Brini, M., Calì, T., Ottolini, D., & Carafoli, E. (2014). Neuronal calcium signaling: Function and dysfunction. *Cell. Mol. Life Sci. Cellular and Molecular Life Sciences, 71*(15), 2787-2814.

Chen, T., Wardill, T. J., Sun, Y., Pulver, S. R., Renninger, S. L., Baohan, A., Schreiter, E. R., Kerr, R. A., Orger, M. B., Jayaraman, V., Looger, L. L., Svoboda, K., & Kim, D. S. (2013). Ultrasensitive fluorescent proteins for imaging neuronal activity. *Nature, 499*(7458), 295.

Chin, D., & Means, A. R. (2000). Calmodulin: A prototypical calcium sensor. *Trends in Cell Biology, 10*(8), 322-328.

Cull-Candy, S., Kelly, L., & Farrant, M. (2006). Regulation of Ca2 -permeable AMPA receptors: Synaptic plasticity and beyond. *Current Opinion in Neurobiology, 16*(3), 288-297.

Eder, A., & Bading, H. (2007). Calcium signals can freely cross the nuclear envelope in hippocampal neurons: Somatic calcium increases generate nuclear calcium transients. *BMC Neuroscience BMC Neurosci, 8*(1), 57.

Emptage, N., Bliss, T. V., & Fine, A. (1999). Single Synaptic Events Evoke NMDA Receptor–Mediated Release of Calcium from Internal Stores in Hippocampal Dendritic Spines. *Neuron, 22*(1), 115-124.

Fedorenko, O. A., & Marchenko, S. M. (2014). Ion channels of the nuclear membrane of hippocampal neurons. *Hippocampus, 24*(7), 869-876.

Gerace, L., & Burke, B. (1988). Functional Organization of the Nuclear Envelope. *Annual Review of Cell Biology Annu. Rev. Cell. Biol., 4*(1), 335-374.

Hagenston, A. M., & Bading, H. (2011). Calcium Signaling in Synapse-to-Nucleus Communication. *Cold Spring Harbor Perspectives in Biology, 3*(11).

Hajnoczky, G., Hager, R., & Thomas, A. P. (1999). Mitochondria Suppress Local Feedback Activation of Inositol 1,4,5-Trisphosphate Receptors by Ca2. *Journal of Biological Chemistry, 274*(20), 14157-14162.

Hakamata, Y., Nakai, J., Takeshima, H., & Imoto, K. (1992). Primary structure and distribution of a novel ryanodine receptor/calcium release channel from rabbit brain. *FEBS Letters, 312*(2-3), 229-235.

Hardingham, G. E., Chawla, S., Johnson, C. M., & Bading, H. (1997). Distinct functions of nuclear and cytoplasmic calcium in the control of gene expression. *Nature, 385*(6613), 260-265.

Hardingham, G. E., L. Arnold, F. J., & Bading, H. (2001). Nuclear calcium signaling controls CREB-mediated gene expression triggered by synaptic activity. *Nature Neuroscience, 4*(3), 261.

Henderson, M. J., Baldwin, H. A., Werley, C. A., Boccardo, S., Whitaker, L. R., Yan, X., Holt, G. T., Schreiter, E. R., Looger, L. L., Cohen, A. E., Kim, D. S., & Harvey, B. K. (2015). A Low Affinity GCaMP3 Variant (GCaMPer) for Imaging the Endoplasmic Reticulum Calcium Store. *PloS One, 10*(10), E0139273.

Henzi, V., & MacDermott, A. (1992). Characteristics and function of Ca2 — and inositol 1,4,5-trisphosphate-releasable stores of Ca2 in neurons. *Neuroscience, 46*(2), 251-273.

Higley, M. J., & Sabatini, B. L. (2012). Calcium Signaling in Dendritic Spines. *Cold Spring Harbor Perspectives in Biology, 4*(4).

Hofmann, F., Lacinová, L., & Klugbauer, N. (n.d.). Voltage-dependent calcium channels: From structure to function. *Reviews of Physiology, Biochemistry and Pharmacology Reviews of Physiology, Biochemistry and Pharmacology, Volume 139,* 33-87.

Johenning, F. W., Theis, A., Pannasch, U., Rückl, M., Rüdiger, S., & Schmitz, D. (2015). Ryanodine Receptor Activation Induces Long-Term Plasticity of Spine Calcium Dynamics. *PLOS Biology PLoS Biol, 13*(6).

Kano, M., Garaschuk, O., Verkhratsky, A., & Konnerth, A. (1995). Ryanodine receptor-mediated intracellular calcium release in rat cerebellar Purkinje neurones. *The Journal of Physiology, 487*(1), 1-16.

Kim, C. K., Miri, A., Leung, L. C., Berndt, A., Mourrain, P., Tank, D. W., & Burdine, R. D. (2014). Prolonged, brain- wide expression of nuclear- localized GCaMP3 for functional circuit mapping. *Frontiers in Neural Circuits, 8*, 138.

Kirichok, Y., Krapivinsky, G., & Clapham, D. E. (2004). The mitochondrial calcium uniporter is a highly selective ion channel. *Nature, 427*(6972), 360-364.

Korkotian, E., & Segal, M. (1998). Fast confocal imaging of calcium released from stores in dendritic spines. *European Journal of Neuroscience, 10*(6), 2076-2084.

Kumar, V., Jong, Y. I., & O'Malley, K. L. (2008). Activated Nuclear Metabotropic Glutamate Receptor mGlu5 Couples to Nuclear $Gq/_{11}$ Proteins to Generate Inositol 1,4,5- Trisphosphate- mediated Nuclear Ca^{2+} Release. *Journal of Biological Chemistry, 283*(20), 14072-14083

Ledeen, R., & Wu, G. (2007). GM1 in the nuclear envelope regulates nuclear calcium through association with a nuclear sodium-calcium exchanger. *Journal of Neurochemistry J Neurochem, 103*(S1), 126-134.

Limback-Stokin, K. (2004). Nuclear Calcium/Calmodulin Regulates Memory Consolidation. *Journal of Neuroscience, 24*(48), 10858-10867.

Lorenzon, P., Zacchetti, D., Codazzi, F., Fumagalli, G., Meldolesi, J., Grohovas, F. (1995). Ca2 waves in PC12 neurites: A bidirectional, receptor-oriented form of Ca2 signaling. *The Journal of Cell Biology, 129*(3), 797-804.

Lui, P. P., Kong, S. K., Fung, K. P., & Lee, C. Y. (1998). The rise of nuclear and cytosolic Ca 2 can be uncoupled in HeLa cells. *Pflügers Archiv European Journal of Physiology, 436*(3), 371-376.

MacLennan, D. H., Rice, W. J., & Green, N. M. (1997). The Mechanism of Ca2 Transport by Sarco(Endo)plasmic Reticulum Ca2 -ATPases. *Journal of Biological Chemistry, 272*(46), 28815-28818.

Magee, J., & Johnston, D. (1995). Synaptic activation of voltage-gated channels in the dendrites of hippocampal pyramidal neurons. *Science, 268*(5208), 301-304.

Marchenko, S. M., Yarotskyy, V. V., Kovalenko, T. N., Kostyuk, P. G., & Thomas, R. C. (2005). Spontaneously active and InsP 3 -activated ion channels in cell nuclei from rat cerebellar Purkinje and granule neurones. *The Journal of Physiology, 565*(3), 897-910.

Mauceri, D., Hagenston, A. M., Schramm, K., Weiss, U., & Bading, H. (2015). Nuclear Calcium Buffering Capacity Shapes Neuronal Architecture. *Journal of Biological Chemistry J. Biol. Chem., 290*(38), 23039-23049.

McPherson, P. S., Kim, Y., Valdivia, H., Knudson, C., Takekura, H., Franzini-Armstrong, C., Coronado, R., & Campbell, K. P. (1991). The brain ryanodine receptor: A caffeine-sensitive calcium release channel. *Neuron, 7*(1), 17-25.

Mermelstein, P. G., Foehring, R. C., Tkatch, T., Song, W. J., Baranauskas, G., & Surmeier, D. J. (1999). Properties of Q- type calcium channels in neostriatal and cortical neurons are correlated with beta subunit expression. *The Journal of Neuroscience : The Official Journal of the Society for Neuroscience, 19*(17), 7268.

Miyakawa, H., Ross, W. N., Jaffe, D., Callaway, J. C., Lasser-Ross, N., Lisman, J. E., & Johnston, D. (1992). Synaptically activated increases in Ca^{2+} concentration in hippocampal CA1 pyramidal cells are primarily due to voltage-gated Ca2 channels. *Neuron, 9*(6), 1163-1173.

Miyamoto, S., Izumi, M., Hori, M., Kobayashi, M., Ozaki, H., & Karaki, H. (2000). Xestospongin C, a selective and membrane-permeable inhibitor of IP3receptor, attenuates the positive inotropic effect of α-adrenergic stimulation in guinea-pig papillary muscle. *British Journal of Pharmacology, 130*(3), 650-654.

Miyazaki, K., & Ross, W. N. (2013). Ca^{2+} Sparks and Puffs Are Generated and Interact in Rat Hippocampal CA1 Pyramidal Neuron Dendrites. *Journal of Neuroscience, 33*(45), 17777-17788.

Nakagawa, T. (2010). The Biochemistry, Ultrastructure, and Subunit Assembly Mechanism of AMPA Receptors. *Molecular Neurobiology Mol Neurobiol, 42*(3), 161-184.

Nakai, J., Ohkura, M., & Imoto, K. (2001). A high signal-to- noise Ca2+ probe composed of a single green fluorescent protein. *Nature Biotechnology, 19*(2), 137-41.

Niggli, V., Sigel, E., & Carafoli, E. (1982). The purified Ca2+ pump of human erythrocyte membranes catalyzes an electroneutral Ca2+- H+ exchange in reconstituted liposomal systems. *The Journal of Biological Chemistry, 257*(5), 2350.

Oceandy, D., Cartwright, E. J., Emerson, M., Prehar, S., Baudoin, F. M., Zi, M., . . . Neyses, L. (2007). Neuronal Nitric Oxide Synthase Signaling in the Heart Is Regulated by the Sarcolemmal Calcium Pump 4b. *Circulation, 115*(4), 483-492.

Ohkura, M., Sasaki, T., Sadakari, J., Gengyo-Ando, K., Kagawa-Nagamura, Y., Kobayashi, C., Ikegaya, Y., Nakai, J., & Baudry, M. (2012). Genetically Encoded Green Fluorescent Ca 2+ Indicators with Improved Detectability for Neuronal Ca 2+ Signals (Superior G-CaMPs for Detection of Neuronal Signals). *7*(12), E51286.

O'Malley, D. M. (1994). Calcium permeability of the neuronal nuclear envelope: Evaluation using confocal volumes and intracellular perfusion. *The Journal of Neuroscience : The Official Journal of the Society for Neuroscience, 14*(10), 5741.

O'Malley, K. L., Jong, Y. I., Gonchar, Y., Burkhalter, A., & Romano, C. (2003). Activation of Metabotropic Glutamate Receptor mGlu5 on Nuclear Membranes Mediates Intranuclear Ca2 Changes in Heterologous Cell Types and Neurons. *Journal of Biological Chemistry, 278*(30), 28210-28219.

Podor, B., Hu, Y., Ohkura, M., Nakai, J., Croll, R., & Fine, A. (2015). Comparison of genetically encoded calcium indicators for monitoring action potentials in mammalian brain by two-photon excitation fluorescence microscopy. *Neurophoton Neurophotonics, 2*(2), 021014.

Power, J. M., & Sah, P. (2002). Nuclear calcium signaling evoked by cholinergic stimulation in hippocampal CA1 pyramidal neurons. *The Journal of Neuroscience: The Official Journal of the Society for Neuroscience, 22*(9), 3454.

Raturi, A., & Simmen, T. (2013). Where the endoplasmic reticulum and the mitochondrion tie the knot: The mitochondria-associated membrane (MAM). *Biochimica Et Biophysica Acta (BBA) - Molecular Cell Research, 1833*(1), 213-224.

Raymond, C. R., & Redman, S. J. (2006). Spatial segregation of neuronal calcium signals encodes different forms of LTP in rat hippocampus. *The Journal of Physiology, 570*(1), 97-111.

Sabatini, B. L., Oertner, T. G., & Svoboda, K. (2002). The Life Cycle of Ca2 Ions in Dendritic Spines. *Neuron, 33*(3), 439-452.

Sandler, V. M., & Barbara, J. G. (1999). Calcium-induced calcium release contributes to action potential-evoked calcium transients in hippocampal CA1 pyramidal neurons. *The Journal of Neuroscience : The Official Journal of the Society for Neuroscience, 19*(11), 4325.

Seymour-Laurent, K. J., & Barish, M. E. (1995). Inositol 1,4,5- trisphosphate and ryanodine receptor distributions and patterns of acetylcholine- and caffeine-induced calcium release in cultured mouse hippocampal neurons. *The Journal of Neuroscience : The Official Journal of the Society for Neuroscience, 15*(4), 2592.

Sharp, A. H., Mcpherson, P. S., Dawson, T. M., Aoki, C., Campbell, K. P., & Snyder, S. H. (1993). Differential immunohistochemical localization of inositol 1,4,5-trisphosphate- and ryanodine- sensitive Ca2+ release channels in rat brain. *The Journal of Neuroscience : The Official Journal of the Society for Neuroscience, 13*(7), 3051.

Shmigol, A., Usachev, Y., Pronchuk, N., Kirishchuk, S., Kostyuk, P., & Verkhratskii, A. (1994). Properties of the caffeine- sensitive intracellular calcium stores in mammalian neurons. *Neurophysiology, 26*(1), 13-20.

Simms, B., & Zamponi, G. (2014). Neuronal Voltage-Gated Calcium Channels: Structure, Function, and Dysfunction. *Neuron, 82*(1), 24-45.

Simons, T. J. (1988). Calcium and neuronal function. *Neurosurgical Review Neurosurg. Rev., 11*(2), 119-129.

Simpson, P. B., Challiss, R. J., & Nahorski, S. R. (1995). Neuronal Ca2 stores: Activation and function. *Trends in Neurosciences, 18*(7), 299-306.

Soler, F., Plenge-Tellechea, F., Fortea, I., & Fernandez-Belda, F. (1998). Cyclopiazonic Acid Effect on Ca 2 -Dependent Conformational States of the Sarcoplasmic Reticulum ATPase. Implication for the Enzyme Turnover †. *Biochemistry, 37*(12), 4266-4274.

Stuart, G. J., & Sakmann, B. (1994). Active propagation of somatic action potentials into neocortical pyramidal cell dendrites. *Nature, 367*(6458), 69-72.

Svoboda, K., Denk, W., Kleinfeld, D., & Tank, D. W. (1997). In vivo dendritic calcium dynamics in neocortical pyramidal neurons. *Nature, 385*(6612), 161-165.

Takeuchi, A., Kim, B., & Matsuoka, S. (2013). The mitochondrial Na -Ca2 exchanger, NCLX, regulates automaticity of HL-1 cardiomyocytes. *Sci. Rep. Scientific Reports, 3*.

Tsai, T. D., & Barish, M. E. (1995). Imaging of caffeine-inducible release of intracellular calcium in cultured embryonic mouse telencephalic neurons. *Journal of Neurobiology J. Neurobiol., 27*(2), 252-265.

Usachev, Y., Shmigol, A., Pronchuk, N., Kostyuk, P., & Verkhratsky, A. (1993). Caffeine-induced calcium release from internal stores in cultured rat sensory neurons. *Neuroscience, 57*(3), 845-859.

Verkhratsky, A. J., & Petersen, O. H. (1998). Neuronal calcium stores. *Cell Calcium, 24*(5-6), 333-343.

Vladimirov, N., Mu, Y., Kawashima, T., Bennett, D. V., Yang, C., Looger, L. L., . . . Ahrens, M. B. (2014). Light- sheet functional imaging in fictively behaving zebrafish. *Nature Methods*.

Wagner, L. E., & Yule, D. I. (2011). Regulation of the Type 1 and Type 2 Inositol 1,4,5-Trisphosphate Receptor Single Channel Open Probability by ATP in On-Nucleus Patch Clamp Recordings. *Biophysical Journal, 100*(3).

Watanabe, S., Hong, M., Lasser-Ross, N., & Ross, W. N. (2006). Modulation of calcium wave propagation in the dendrites and to the soma of rat hippocampal pyramidal neurons. *The Journal of Physiology, 575*(2), 455-468.

Westenbroek, R. E., Ahlijanian, M. K., & Catterall, W. A. (1990). Clustering of L-type Ca2 channels at the base of major dendrites in hippocampal pyramidal neurons. *Nature, 347*(6290), 281-284.

Yasuda, R., Sabatini, B. L., & Svoboda, K. (2003). Plasticity of calcium channels in dendritic spines. *Nature Neuroscience Nat Neurosci, 6*(9), 948-955.

Zalk, R., Lehnart, S. E., & Marks, A. R. (2007). Modulation of the Ryanodine Receptor and Intracellular Calcium. *Annu. Rev. Biochem. Annual Review of Biochemistry, 76*(1), 367-385.

Zhang, S., Steijaert, M. N., Lau, D., Schütz, G., Delucinge-Vivier, C., Descombes, P., & Bading, H. (2007). Decoding NMDA Receptor Signaling: Identification of Genomic Programs Specifying Neuronal Survival and Death. *Neuron, 53*(4), 549-562.

Zhang, S., Zou, M., Lu, L., Lau, D., Ditzel, D. A., Delucinge-Vivier, C., . . . Bading, H. (2009). Nuclear Calcium Signaling Controls Expression of a Large Gene Pool: Identification of a Gene Program for Acquired Neuroprotection Induced by Synaptic Activity. *PLoS Genetics PLoS Genet, 5*(8).